NAVAL POSTGRADUATE SCHOOL

MONTEREY, CALIFORNIA

THESIS

PROPAGATION MODELING OF WIRELESS SYSTEMS IN SHIPBOARD COMPARTMENTS

by

Adnen Chaabane

March 2005

Thesis Advisor:	David C. Jenn
Co- Adviser:	Curt D. Schleher

Approved for public release; distribution is unlimited

THIS PAGE INTENTIONALLY LEFT BLANK

REPORT DOCUMENTATION PAGE			Form Approved OMB No. 0704-0188
Public reporting burden for this collection of information is estimated to average 1 hour per response, including the time for reviewing instruction, searching existing data sources, gathering and maintaining the data needed, and completing and reviewing the collection of information. Send comments regarding this burden estimate or any other aspect of this collection of information, including suggestions for reducing this burden, to Washington headquarters Services, Directorate for Information Operations and Reports, 1215 Jefferson Davis Highway, Suite 1204, Arlington, VA 22202-4302, and to the Office of Management and Budget, Paperwork Reduction Project (0704-0188) Washington DC 20503.			
1. AGENCY USE ONLY ***(Leave blank)***	**2. REPORT DATE** March 2005	**3. REPORT TYPE AND DATES COVERED** Master's Thesis	
4. TITLE AND SUBTITLE: Propagation Modeling of Wireless Systems in Shipboard Compartments			**5. FUNDING NUMBERS**
6. AUTHOR(S) Adnen Chaabane			
7. PERFORMING ORGANIZATION NAME(S) AND ADDRESS(ES) Naval Postgraduate School Monterey, CA 93943-5000			**8. PERFORMING ORGANIZATION REPORT NUMBER**
9. SPONSORING /MONITORING AGENCY NAME(S) AND ADDRESS(ES) N/A			**10. SPONSORING/MONITORING AGENCY REPORT NUMBER**
11. SUPPLEMENTARY NOTES The views expressed in this thesis are those of the author and do not reflect the official policy or position of the Department of Defense or the U.S. Government.			
12a. DISTRIBUTION / AVAILABILITY STATEMENT Approved for public Release; distribution is unlimited			**12b. DISTRIBUTION CODE** A

13. ABSTRACT (maximum 200 words)

In today's navy, it is becoming more and more important to reach all areas onboard a ship with key technical resources. In order to accomplish this goal, the already existing physical networks need to be complemented with wireless capability. A sophisticated Wireless Local Area Network (WLAN) can provide that vital connectivity to the ship's network resources from almost anywhere on the ship. It would allow sailors to access critical information and immediately communicate with others throughout the ship from any standard wireless device (PDA, laptop and many other hand-held devices). In addition, WLANs greatly mitigate problems due to physical damage to wires or fiber optic cables that are used today. Because the navy's emphasis is on building ships with reduced manning, advanced technology, and lower cost in mind, the idea of a WLAN, which has a deep impact on all those areas, has been of a growing interest to the Navy.

The purpose of this thesis is to analyze, model, and simulate a wireless environment on board a variety of naval ship compartments, using the Urbana code. Starting from known inputs (frequency, ship compartment geometry, material properties, propagation computation model, and antenna type), analytical results reflecting the propagation mechanisms, coverage area, and security posture of the WLAN are presented. Variable inputs can then be optimized to achieve a desired signal distribution and to meet security requirements for a specific shipboard environment.

14. SUBJECT TERMS Simulation of Wireless Propagation, Shipboard Modeling, Antenna Propagation, Urbana, Wireless Security, Indoor Propagation, Indoor-Outdoor Propagation			**15. NUMBER OF PAGES** 115
			16. PRICE CODE
17. SECURITY CLASSIFICATION OF REPORT Unclassified	**18. SECURITY CLASSIFICATION OF THIS PAGE** Unclassified	**19. SECURITY CLASSIFICATION OF ABSTRACT** Unclassified	**20. LIMITATION OF ABSTRACT** UL

NSN 7540-01-280-5500 Standard Form 298 (Rev. 2-89)
Prescribed by ANSI Std. 239-18

THIS PAGE INTENTIONALLY LEFT BLANK

Approved for public release; distribution is unlimited

PROPAGATION MODELING OF WIRELESS SYSTEMS IN SHIPBOARD COMPARTMENTS

Adnen Chaabane
Lieutenant Junior Grade, Tunisian Navy
B.S., United States Naval Academy, 2000

Submitted in partial fulfillment of the
requirements for the degree of

MASTER OF SCIENCE IN ELECTRICAL ENGINEERING
and
MASTER OF SCIENCE IN SYSTEMS ENGINEERING

from the

NAVAL POSTGRADUATE SCHOOL
March 2005

Author:

Adnen Chaabane

Approved by:

David C. Jenn,
Thesis Advisor

Curt D. Schleher
Co-Advisor

Dan Boger,
Chairman, Department of Information Sciences

John Powers,
Chairman, Department of Electrical and Computer Engineering

THIS PAGE INTENTIONALLY LEFT BLANK

ABSTRACT

In today's navy, it is becoming more and more important to reach all areas on-board a ship with key technical resources. In order to accomplish this goal, the already existing physical networks need to be complemented with wireless capability. A sophisticated Wireless Local Area Network (WLAN) can provide that vital connectivity to the ship's network resources from almost anywhere on the ship. It would allow sailors to access critical information and immediately communicate with others throughout the ship from any standard wireless device (PDA, laptop and many other hand-held devices). In addition, WLANs greatly mitigate problems due to physical damage to wires or fiber optic cables that are used today. Because the navy's emphasis is on building ships with reduced manning, advanced technology, and lower cost in mind, the idea of a WLAN, which has a deep impact on all those areas, has been of a growing interest to the Navy.

The purpose of this thesis is to analyze, model, and simulate a wireless environment on board a variety of naval ship compartments, using the Urbana code. Starting from known inputs (frequency, ship compartment geometry, material properties, propagation computation model, and antenna type), analytical results reflecting the propagation mechanisms, coverage area, and security posture of the WLAN are presented. Variable inputs can then be optimized to achieve a desired signal distribution and to meet security requirements for a specific shipboard environment.

THIS PAGE INTENTIONALLY LEFT BLANK

TABLE OF CONTENTS

THIS PAGE INTENTIONALLY LEFT BLANK

LIST OF FIGURES

LIST OF TABLES

THIS PAGE INTENTIONALLY LEFT BLANK

ACKNOWLEDGMENTS

I would like to express my sincere thanks to Professor David Jenn for his support, guidance, and advice during the research and completion of this thesis. Additional thanks are extended to Professor Curtis Schleher for his help and assistance. I would also like to thank my parents for their continuous support from thousands of miles away all along this research effort. Finally, I extend special thanks to my wife, Olfa, and my dear son, Adam, who have always motivated me, encouraged me, and supported me in every way they could.

THIS PAGE INTENTIONALLY LEFT BLANK

EXECUTIVE SUMMARY

As the ships of the Navy become more technologically advanced and less manned, the need to utilize valuable personnel and sensor resources has become more imperative. In a ship environment, the crew demand mobility and need to reach remote areas where crucial network resources may not be accessible with a standard wired network. The recent advances in wireless networking offer a solution for the connectivity to the ship's network resources from virtually all spaces on the ship. Laptops, standard wireless PDAs, and other hand-held devices connected to a ship WLAN can be used by the crew to supplement rapid and concrete damage control reports, to make instantaneous log entries into a central data base, and to communicate with others throughout the ship. WLAN capabilities greatly improve the situational awareness and efficiency of the ship team and offer a significant supplement to the wired local area network.

Because wireless signals travel in free space and may expand beyond the defined boundaries of a ship, they are vulnerable to eavesdropping and intentional interference. These signals can be intercepted by unwanted users who could collect sensitive information and disrupt the network. In a military environment, security is paramount; therefore a careful examination of how and where signals propagate is necessary.

This thesis serves as part of an ongoing evaluation of the feasibility of shipboard wireless networks. The primary objective of this thesis was to investigate the propagation of wireless signals in some typical shipboard compartments. The Urbana software package was used as the simulation tool.

Because the focus of this research was on a simple site specific description of a shipboard environment, a variety of models for shipboard compartments are developed in Chapter V. Most models were developed with the Rhino software, but some were built with the Cifer application in Urbana. In Chapter VI, some simple examples are developed to assess the performance of the Urbana code and to validate its use in complex and challenging propagation environments. Then, an analysis of the different possible input

parameters to the Urbana input file is conducted. Finally, based on the results of that analysis, a selection of the best input parameters that fit the application of implementing WLANs onboard ships is made.

In Chapter VII, a series of simulations are conducted to assess the signal distribution inside and outside of the compartment models developed in Chapter V and to evaluate the security posture of the network. Each simulation starts with known inputs of the antenna (frequency, location, emitted power and radiation pattern), the specifications of the environment (like the structure geometry and material properties), and the propagation computation model. The simulation results depict the signal distribution over a plane of observation points (representing the location of possible receiving devices), from which the security posture of the WLAN is surmised.

The output results of Urbana show that this simulation code is a very useful tool for the propagation modeling of wireless waves in shipboard compartments. A network designer can optimize the antenna location, pattern and effective radiated power, and some of the environment characteristics (like the material properties and opening positions), to achieve a required signal distribution level in specific areas. The most useful aspect of computer simulation is its ability to answer the question: “what happens if one or a number of the input variables are changed?” By providing the user with the signal strength at specific observation points, these simulations help designers assess the performance of a WLAN.

The simulation results of this thesis show that Urbana can be used to predict the security posture of a network. Based on the spread of the signal level in regions beyond the desired boundaries of an area network (because of openings, material properties of the environment, or power level used), some security measures can be taken to improve the operation of wireless networks on board ships. These measures include:

- Locating access points as far from the openings as possible.
- Putting the transmitting antenna in the most interior and physically secure parts of the ship.
- Using sectored access points to limit the spatial radiation distribution.

- Closing all hatches and doors when propagation outside a single compartment is to be avoided.
- Decreasing the amount of radiated power if that is over and above the required signal level.
- Using perfect electric conductor material for outside walls and for doors and hatches because EM waves do not propagate through PEC material.
- Changing some of the material properties of the environment in order to either achieve a better coverage area inside a compartment or to improve security while maintaining the same radiated power level.

THIS PAGE INTENTIONALLY LEFT BLANK

I. INTRODUCTION

A. WIRELESS VS WIRED APPLICATIONS

In 1985, the Federal Communications Commission (FCC) enabled the development of commercial wireless LANs by authorizing the public use of the Industrial, Scientific, and Medical (ISM) frequency bands for wireless LAN products without a license. Because of interference problems with the primary ISM band users, wireless LANs had to use a low power profile (a maximum of 36 dBm of effective radiated power (ERP) for most applications). During the last couple of years, WLANs have seen a big growth to the point that organizations require WLANs to conduct normal day-to-day business. By connecting devices and promoting wireless computing technologies, it has become possible to connect remote, hard to reach, and mobile assets in a cost effective, secure, and reliable manner.

The soaring growth of wireless solutions with increasing throughput characteristics that can support data-intensive applications, coupled with the proliferation of laptop and palmtop computers indicate an even brighter future for wireless networks [1]. Such solutions have already achieved improvements in security and emergency response, management of resources, optimization of logistics, and mobility and collaboration. Also, wireless sensor networking provides the opportunity to collect real-time information that may be used to measure an almost unlimited set of parameters and monitor previously inaccessible devices and locations.

The advantages of WLANs for the Navy include ease of installation and use, improved system reliability and monitoring, technology integration, flexibility, and mobility. With a declining cost and improving technology and infrastructure, the deployment of wireless applications is quickly increasing while the deployment of wired systems is holding steady if not decreasing.

B. KEY ATTRIBUTES OF WIRELESS STANDARDS

1. Evolution of Wireless Networks

a. Point-to-Point

Wireless networks first started as a point-to-point application where there had to be a direct connection between devices as is shown in Figure 1. The wireless link in this case is basically a simple wire replacement and has limited communication and expandability capabilities.

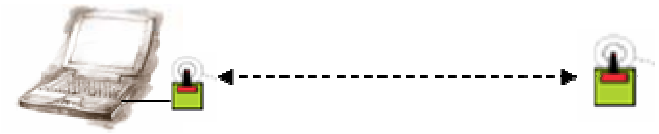

Figure 1. Point-to-point wireless architecture

b. Point-to-Multipoint

The point-to-multipoint network architecture is characterized by a centralized routing and control point where all data must flow through a "base station" as is shown in Figure 2. The IEEE 802.11 standard (also known as the Wi-Fi standard), and the GSM cellular network, are examples of this wireless architecture.

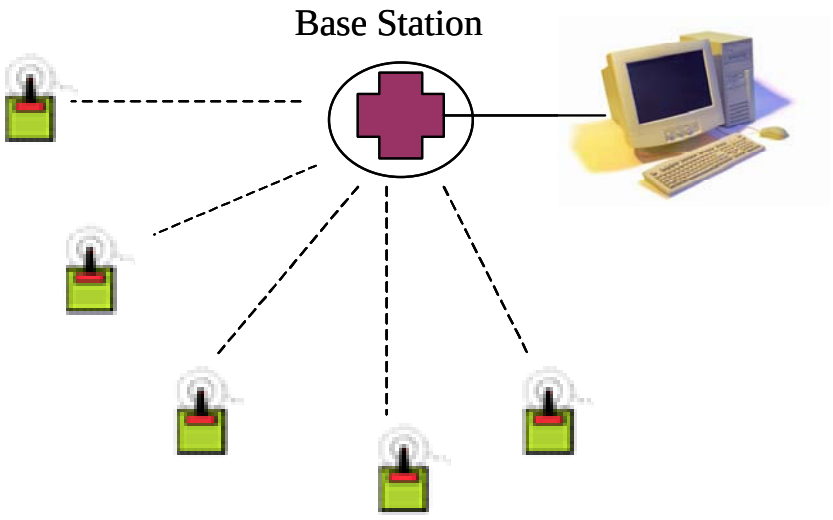

Figure 2. Point-to-multipoint architecture

c. Mesh

The mesh architecture is characterized by a full radio frequency (RF) redundancy with multiple data paths. The network is considered self-configuring or self-healing with distributed intelligence. No centralized control is required to maintain the network. This type of network is used in the IEEE 802.15.4 standard (also known as ZigBee). Figure 3 shows an example of a mesh network.

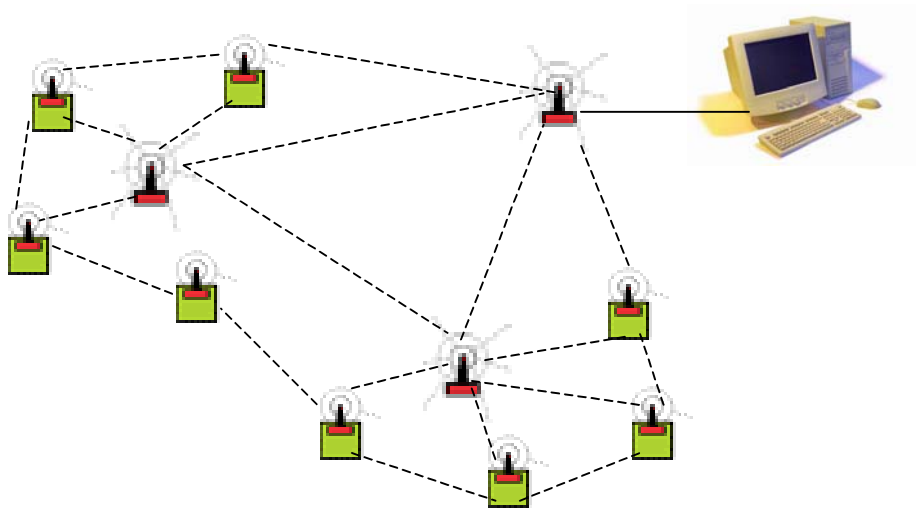

Figure 3. Mesh architecture

2. Key Attributes of Current Wireless Standards

Wireless use includes a wide range of applications that vary from voice, internet access, messaging, and file transfer, to video teleconferencing, remote control, local area networking, and sensing. These different applications have different requirements. Voice systems require low data rates, can tolerate high probability of bit error, but require a very low delay time. Video teleconferencing requires a high throughput with the same delay constraints as voice systems. On the other hand, messaging and some data applications require only low data rates and almost no delay time constraints. These application-dependent requirements make it hard to find a single wireless standard that concurrently satisfies all types of requirements. As a matter of fact, such solution would have to meet the most severe requirements from each application, which implies to very high data rates (in the Gbps), and very low bit error rates (as low as 10^{-12}). Because a solution is not fea-

sible using today's technology, wireless systems will continue to have different protocols tailored to support specific applications.

Table 1 summarizes the key attributes of current wireless standards. Depending on the required range, bandwidth and system resources, a user can decide on the best standard that fits a specific application.

Market Name **Standard**	*Cellular Network* **GSM/CDMA**	*Wi-Fi* **802.11a/b/g**	*Bluetooth* **802.15.1**	*ZigBee* **802.15.4**
Application Focus	Cellular telephones Telemetry	LAN, Internet	Cable Replacement	Sensor Networks
Modulation	CDMA/GSM/AMPS	DSSS/OFDM	Adaptive FHSS	DSSS
Frequency Range	869-894 MHz	2.4 GHz-b/g 5.8 GHz-a	4 GHz	868/915 MHz 2.4 GHz
Network Size **Network Type**	1 IP	32 IP & P2P	7 P2P	65000 Mesh
Bandwidth (kB/s)	64-128+	11000+	720	20-250
Transmission Range (m)	1000+	100	10	70-100+
Success Metrics	Reach, Quality	Speed, Flexibility	Cost, Convenience	Reliability, Power, Cost

Table 1. Key attributes of current wireless standards

Figure 4 [2] shows a plot of data rate versus range for current wireless standards. It is clear that the ZigBee standard and the IEEE 802.15.1 standard (also known as Bluetooth) are low data rate networks (below 1 Mbps), while the IEEE 802.11 standard can offer a throughput as high as 54 Mbps.

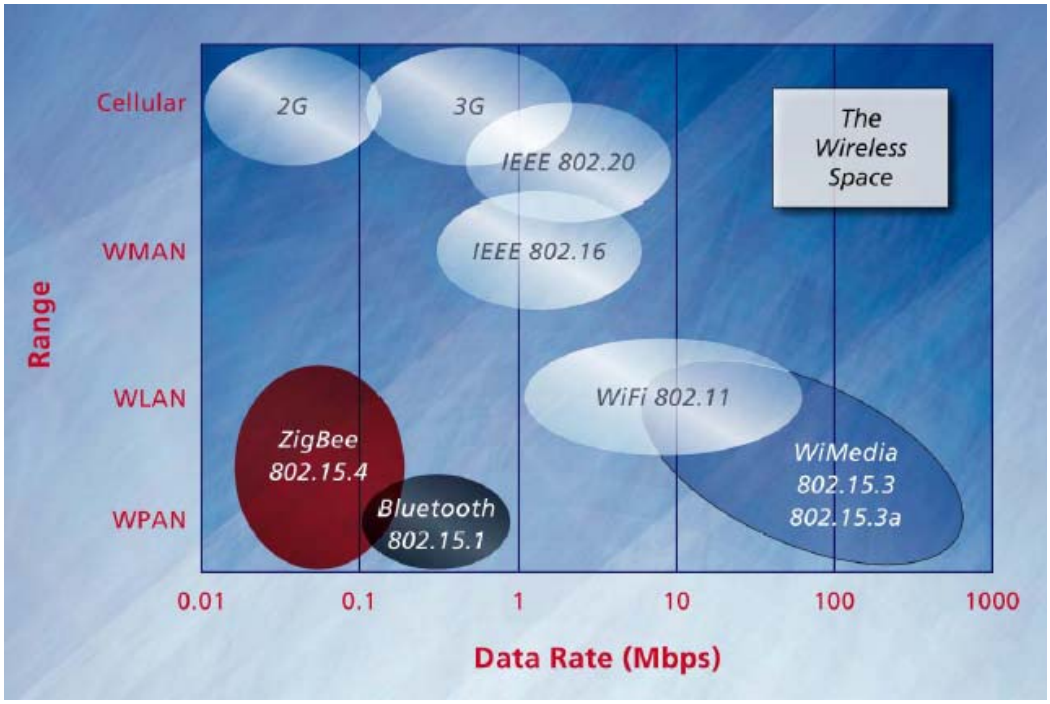

Figure 4. Range vs data rate for the most common wireless standards [From Ref. 2.]

Depending on the objective at hand, the ZigBee, Bluetooth and Wi-Fi standards are all possible solutions for wireless applications on board ships. Each of these standards is analyzed in the next sections of this chapter.

3. Bluetooth Standard

The Bluetooth standard is basically a cable-replacement technology for short range connections between wireless devices. Its normal range of operation is 10 m at a power of 1 mW. It is a good solution for a peer-to-peer application (like a wireless connection between two devices on the bridge of a ship). Because the purpose of this thesis is the study of a WLAN that can cover a full compartment or a number of compartments onboard a ship, it is clear that the Bluetooth technology does not meet the functionality and range requirements of such application.

4. ZigBee Standard

The ZigBee standard operates in the 868-MHz, 915-MHz and 2.4-GHz bands. It is the global standard for low data rate networks that require transmission ranges between 30 to 100 m (single hop). The ZigBee standard is ideal for closed control networks like the one found on naval vessels. It is well suited for naval applications that require the monitoring and control of a network of sensors (like the ones found in the engine room or any other control station). High data reliability, security (achieved through a 128-bit encryption), advanced power management, and protocol simplicity are some of the key features for this type of network. Figure 5 depicts a possible layout of the ZigBee network onboard a naval vessel.

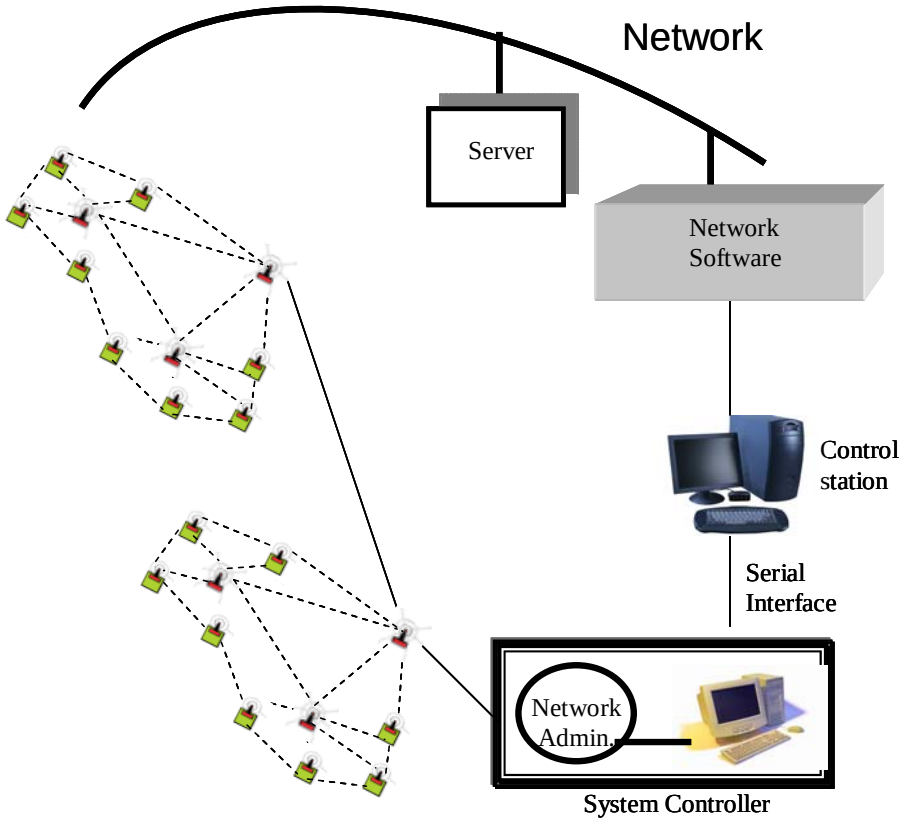

Figure 5. ZigBee standard

5. Wi-Fi Standard

The IEEE 802.11 standard offers data rates up to 54 Mbps. With a transmission range of 100 m, this standard is perfect for naval wireless applications that require a high bandwidth and are intra- or Internet and browser based, rather than sensor network based. The standard is based on an IT interface that requires access points and hot spots. This protocol is widely used in the industry today and has shown good reliability, security, and ease of integration and deployment. Figure 6 shows a possible configuration of a Wi-Fi network.

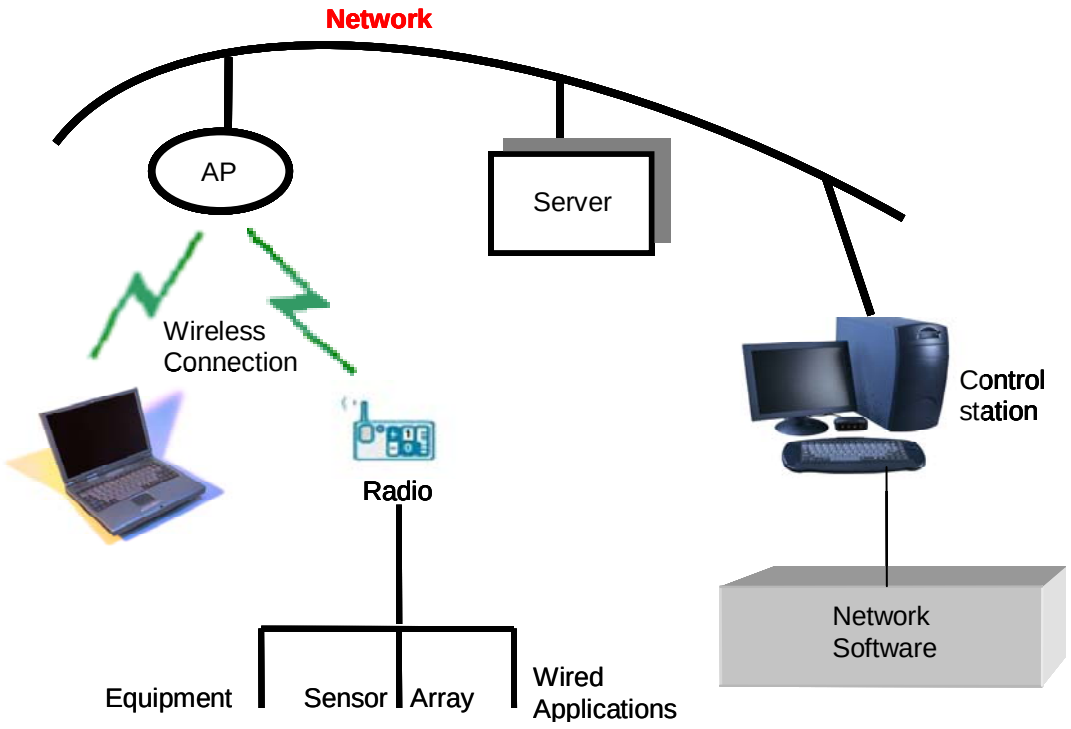

Figure 6. Wi-Fi standard

6. Shipboard WLAN

In a ship environment, wireless applications can make use of one or several of the above standards as shown in Figure 7. Depending on the data rate requirements, as well as the bandwidth and range constraints, an engineer can choose the best standard that fits a specific application.

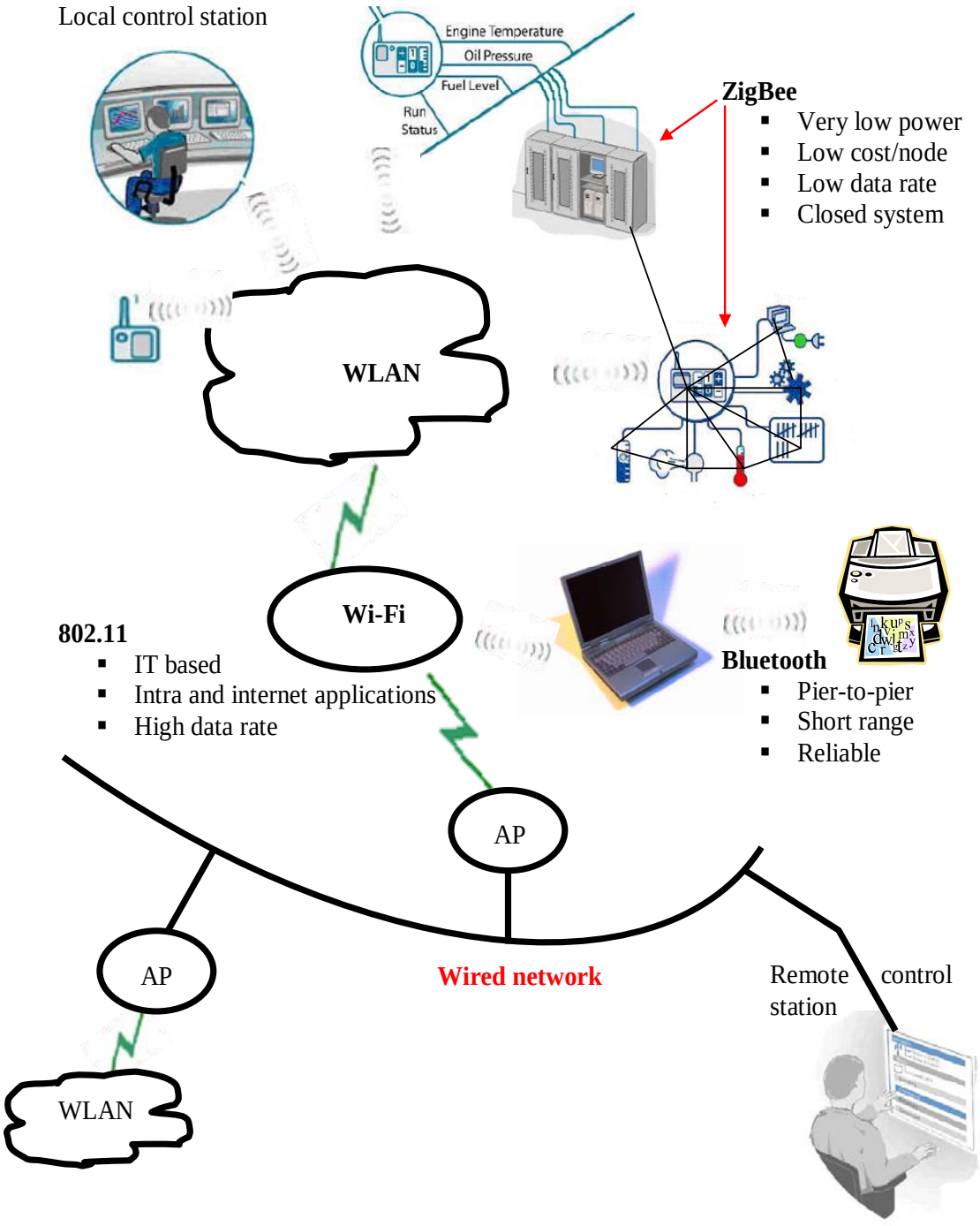

Figure 7. Possible wireless applications onboard ships

C. WIRELESS NETWORK SECURITY

Because WLANs use radio frequency waves that propagate in free space, they are susceptible to interception and manipulation. In addition, it is possible that high power signals can be injected into the ship's network to jam or incapacitate it. Once inside the network, deceptive signals can be easily inserted to cause confusion and disorder.

There are only two ways to prevent such a breach in the network security. The first method is to limit the signal coverage to a physically defined secure zone that intruders and unwanted users can not reach. This requires a good knowledge of how waves propagate and how they interact with their environment, which is the subject of this research. By knowing the precise spread of the network coverage area and the possible receiver sensitivities that unwanted intruders might possess, it becomes relatively easy, and more efficient, to allocate resources in order to protect and guard areas of hot spots where the signal level is high enough to be intercepted.

The second method is to prevent access to the network for unauthorized users even if they can reach it. This can be accomplished by implementing a variety of security features into the network's operating system. The Wired Equivalent Privacy (WEP) algorithm [3] designed to provide privacy of transmitted data between the wireless client and the access point, and the Media Access Control (MAC) procedure (where address based access lists on access points are used to register and recognize MAC addresses that are allowed to join a network), are some of those security measures. As shown in [3], these measures have been effective against immature hackers, but can be defeated by crackers or knowledgeable hackers.

In a military environment, both methods have to be implemented simultaneously and rigorously in order to lower the probability of interception and manipulation of the network signals. The simulation results of this thesis lead to simple but effective steps that could improve the security posture of a network by limiting its coverage area to a desirable protected zone.

D. OBJECTIVE AND APPROACH

Because wireless technology decision dictates the knowledge of coverage range, availability, and security, based on the characteristics of the environment, transmitter and receiver, the focus of this thesis is to assess the performance of a WLAN in a shipboard setting in all of the above mentioned areas.

One goal is to evaluate the use of the Urbana code to assess the performance of WLANs on board naval vessels. Although the Bluetooth and the ZigBee standards have shown their usefulness in shipboard wireless applications, only the IEEE 802.11 standard meets the functional and range requirements to be used in the implementation of a WLAN on board a ship. The results presented in this research reflect only simulations of the 802.11b (2.4 GHz) industry standard network. The simulation starts with the known inputs of a specific access point (frequency, location, emitted power and antenna type), the ship geometry and material properties, and the propagation computation model. The simulation output result depicts the signal distribution over a plane of observation points (representing possible locations of receiving devices), from which the security posture of the WLAN can be inferred.

E. THESIS OUTLINE

This thesis is organized as follows. Chapter II discusses important background information that relates to wireless wave propagation. Chapter III presents the different types of indoor models that have been developed in order to simulate the behavior of wireless waves in an indoor setting. Chapter IV gives an overview of the Urbana software used to perform the simulations, while Chapter V describes how the different models of shipboard compartments were developed for this thesis.

Chapter VI discusses the selection of the different input parameters used in the simulations. In Chapter VII, a thorough simulation and analysis of a WLAN implementation on board a variety of naval compartments is conducted. Chapter VIII summarizes the results of this thesis and gives recommendations for future work.

II. BACKGROUND

The previous chapter described the different wireless standards and their key attributes, and introduced the challenges that face network security. This chapter explains how electromagnetic (EM) waves propagate and introduces important background information that relates to wireless propagation.

In addition to describing the fundamentals of antenna theory, this chapter identifies the key principles of EM propagation: attenuation in bulk material, scattering, and interference.

A. PHYSICS OF PROPAGATION

1. Electromagnetic Radiation

Electromagnetic radiation consists of simultaneously oscillating electric and magnetic fields that are coupled as described by Maxwell's equations:

$$\nabla \times \vec{E} = -\frac{\partial \vec{B}}{\partial t} \tag{1}$$

$$\nabla \times \vec{H} = \frac{\partial \vec{D}}{\partial t} + \vec{J} \tag{2}$$

$$\nabla \cdot \vec{D} = \rho \tag{3}$$

$$\nabla \cdot \vec{B} = 0 \tag{4}$$

where $\vec{E}$ (V/m) is the electric field intensity, $\vec{D}$ (C/m^2) is the electric displacement, $\vec{B}$ (T) is the magnetic flux, $\vec{H}$ (A/m) is the magnetic field intensity, ρ (C/m^3) is the charge density, and $\vec{J}$ (A/m^2) is the current. From this point, we assume time-harmonic fields with a $e^{j\omega t}$ time dependence and use phasors notation.

Before proceeding, it is necessary to introduce the constitutive parameters that relate the intensities to the densities:

$$\vec{D} = \varepsilon \vec{E} \tag{5}$$

$$\vec{B} = \mu \vec{H} \tag{6}$$

$$\vec{J} = \sigma \vec{E} \tag{7}$$

where ε, μ, and σ are, respectively, the permittivity, permeability and conductivity of the medium through which the waves are propagating. Complex ε and μ, along with σ, completely describes a material

$$\varepsilon = \varepsilon' - j\varepsilon'' \tag{8}$$

$$\mu = \mu' - j\mu'' . \tag{9}$$

The relative values are defined as:

$$\varepsilon = \varepsilon_0 \varepsilon_r = \varepsilon_0 \left(\varepsilon_r' - j\varepsilon_r'' \right) \tag{10}$$

$$\mu = \mu_0 \mu_r \tag{11}$$

where ε_r' and ε_r'' are the real and imaginary parts of the relative permittivity ε_r of the material and $\varepsilon_0 = 8.8542 \times 10^{-12}$ (F/m) is the free space permittivity. Because the majority of the materials in an indoor setting are nonmagnetic, it is assumed that $\mu_r = 1$, and $\mu = \mu_0 = 4\pi \times 10^{-7}$ (H/m) . The intrinsic impedance of the medium is

$$\eta = \sqrt{\mu / \varepsilon} . \tag{12}$$

Assuming that the region of space of interest is source free (charge density and current density are zero), Maxwell's equations can be solved to yield the wave equation for the electric field:

$$\nabla^2 \vec{E} + k^2 \vec{E} = 0 \tag{13}$$

where $k = \omega\sqrt{\mu\varepsilon} = 2\pi/\lambda$, $\omega = 2\pi f$, f is the frequency, and λ is the wavelength ($= c/f$).

The most elementary solutions of the wave equation are plane waves

$$\vec{E} = \vec{E}_0 e^{\pm j\vec{k}\cdot\vec{r}} \tag{14}$$

where $\vec{E}_0$ is the electric field at the source, $\vec{k}$ is a vector in the direction of propagation, and $\vec{r}$ is a position vector from the origin to the point (*x, y, z*) where the electric field is evaluated [4].

The wave equation admits other solutions, among them are spherical waves. A spherical wave may be represented as

$$\vec{E} = \vec{E}_0 \frac{e^{jkr}}{r}. \tag{15}$$

As is illustrated by Equation (15), the electric field strength falls off inversely with the radial distance r from the point where propagation is initiated. The power carried by the wave spreads as $1/r^2$ (the inverse square law). In addition, the wave is also subject to attenuation (energy dissipated inside a material) and scattering as it interacts with objects. It can also interact with other waves through the process of interference.

2. Attenuation of Electromagnetic Radiation in Bulk Materials

As waves propagate through a lossy medium, energy is extracted from the wave and absorbed by the medium. The three main sources of loss are ohmic loss (due to the collision of free charges in a conductor), dielectric loss (due to the polarization of molecules caused by an external electric field), and magnetic loss (due to the magnetization of the molecules caused by an external magnetic field) [5].

The time averaged power density of electromagnetic radiation is

$$\vec{w} = \frac{1}{2}\mathrm{Re}\left\{\vec{E} \times \vec{H}^*\right\} = \frac{\left|\vec{E}\right|^2}{2\eta} = \frac{\left|\vec{E}_0\right|^2}{2\eta}\frac{e^{-2\alpha r}}{r^2} \tag{16}$$

where $\vec{E}_0$ is the field at the reference and α is the field attenuation coefficient that determines the rate of decay of the wave. The value of the attenuation coefficient has been tabulated for different materials at different wavelengths in many technical literature books.

3. Scattering

When an incident electromagnetic wave impinges into a surface of a material or meets an obstacle, it can either go through it after a process of refraction which leads to a transmitted wave or scatter. The main scattering mechanisms that are encountered in an indoor environment are reflection and diffraction. Figure 8 shows a case where a transmitted wave gets scattered and partially transmitted after it hits an obstacle.

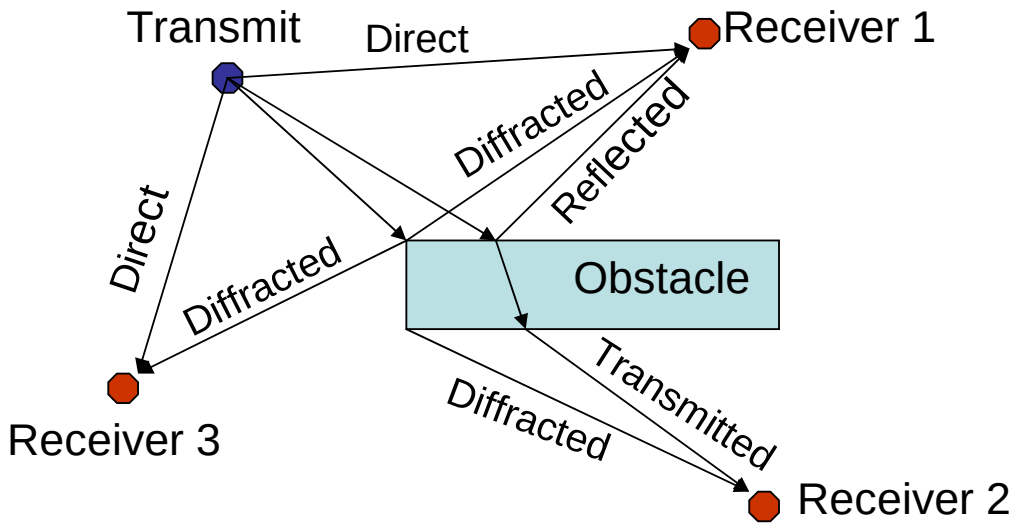

Figure 8. Scattering mechanisms

a. Reflection and Transmission

When an electromagnetic wave is incident on an interface between two media with different characteristics, some of the radiation is reflected by the interface, while some is transmitted through it. The direction of propagation of the transmitted wave is altered through a process called refraction. For a panel in free space, the reflected wave leaves the interface at the same angle θ_i relative to the normal as the incident wave arrives.

The angle of the transmitted wave in the panel is related to the angle of the incident ray by the Snell's law of refraction:

$$\sin\theta_t = \frac{n_1}{n_2}\sin\theta_i \tag{17}$$

where n_1 and n_2 are the refractive indices of the two media as shown in Figure 9. The index of refraction for a medium n is related to the relative permittivity by

$$n = \sqrt{\varepsilon_r}\,. \tag{18}$$

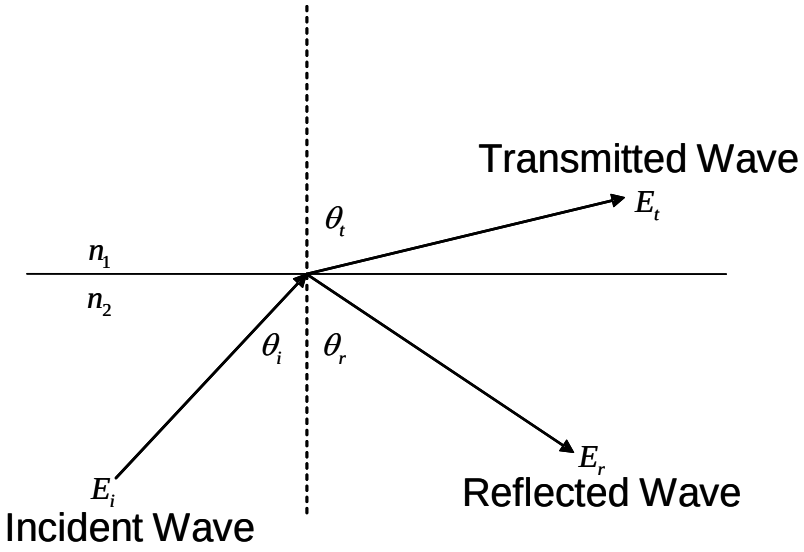

Figure 9. Reflected and transmitted waves

The amplitude of the wave reflected from a perfect electric conductor (PEC) suffers no reduction as none of the energy is transmitted. For dielectrics, the reflection coefficient is

$$\Gamma = \frac{n_1 - n_2}{n_1 + n_2} \tag{19}$$

which relates the incident and reflected fields:

$$E_r = \Gamma E_i \,. \tag{20}$$

b. Diffraction

Diffracted waves are those scattered from discontinuities such as edges and tips. Although most diffracted waves are less intense than reflected waves, they can scatter over a wide range of angles. Because these diffracted waves carry electromagnetic energy in many directions, they make it possible for waves to reach shadow areas that neither direct nor reflected waves could reach. Figure 10 shows diffracted waves off a tip of a wedge. Similar to the case of reflection, a diffraction coefficient D can be defined that relates the incident and reflected fields

$$E_d = DE_i. \tag{21}$$

Formulas are available for computing D for various discontinuities [4].

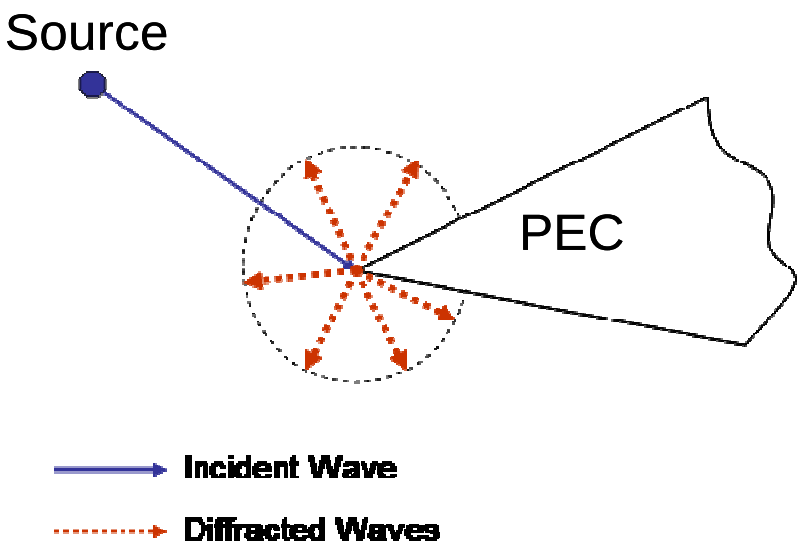

Figure 10. Diffracted waves off a tip of a edge

The total filed at an observation point is the sum of all direct, scattered (reflected, and diffracted) and transmitted fields arriving at that point.

4. Interference

Two electromagnetic waves can interfere with each other. The amplitude at any point in space is equal to the absolute value squared of the total local electric field. Because the local field is the vector sum of all electric fields reaching that point from all contributing sources, the intensity of the electromagnetic radiation can greatly vary depending on the location of the point with respect to other emitting sources. Interference can lead to signals higher than the direct path component when EM waves add, and to very low signal levels when they cancel (fading). This is a crucial problem for naval ships where sources of interference are everywhere for all frequency bands.

B. ANTENNA FUNDAMENTALS

Antennas are devices that excite or sense energy in the environment. In doing so, they perform three main functions:

1) Provide a match between the impedance of the transmission line, waveguide or any other connecting device, and the impedance of the space where they are emitting or sensing.

2) Provide antenna gain relative to an isotropic radiator by collimating or collecting the radiation into a beam that focuses the EM energy.

3) Provide a means of pointing the beam in specific directions (scanning).

Antennas perform these tasks both when transmitting as well as when receiving [6].

1. Antenna Gain

The gain of an antenna is a measure of the ability of the antenna to focus radio waves in a particular direction as compared to an isotropic reference element. In practice, the gain of an antenna can be determined from its effective area A_e and the wavelength λ by

$$G = \frac{4\pi A_e}{\lambda^2}. \tag{22}$$

For an efficient antenna with a well-defined physical aperture area *A*, one can use $A_e \approx A$.

2. Antenna Polarization

The nature of the antenna polarization depends on the path that the tip of $\vec{E}$ traces as the EM wave travels in space. The most general case is elliptical, where both vertical and horizontal field components are present with arbitrary amplitude and phase relationship [7]. Most commercial wireless systems are designed to operate with linear polarization, usually vertical with respect to the ground.

3. Antenna Pattern Characteristics

The radiation pattern represents the antenna radiated (or received) power as a function of angle at a fixed radius from a receiving (or transmitting) antenna. When receiving, an antenna responds to an incoming wave from a given direction according to the pattern value in that direction. Figure 11 [8], illustrates some important antenna pattern characteristics for a typical plot. The figure shows the antenna main lobe, the half-power beamwidth defined at the half-power points and the beamwidth between fist nulls.

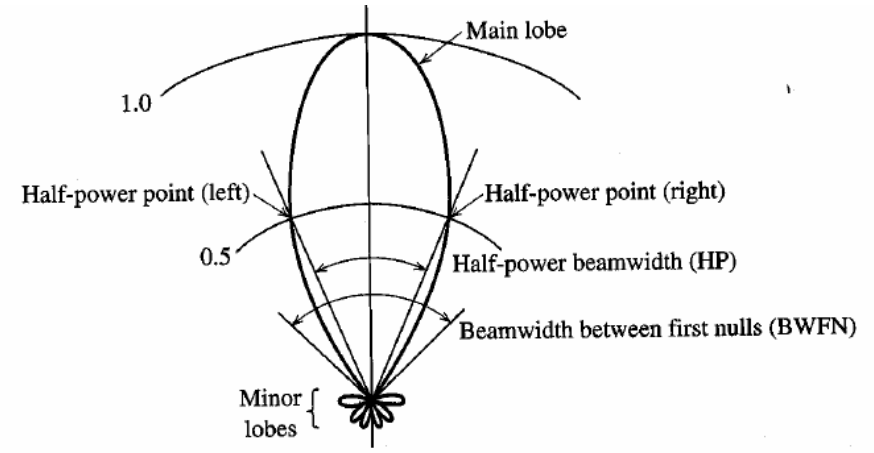

Figure 11. Antenna Pattern Characteristics [From Ref. 8.]

A vertical half-wave dipole antenna, which has an omni-directional footprint in the horizontal plane, is the most common omni-directional antenna of choice. Parabolic type reflectors or arrays are used when it is necessary to direct the transmitted energy into a specific direction with a narrow beam. In this thesis, both directional and omni-directional antennas are considered.

C. CONCLUSION

As illustrated by the discussion in this chapter, electromagnetic waves propagate through environments where they are reflected and diffracted by walls, terrain, buildings, and other objects. The ultimate understanding of the way these waves propagate can be obtained by solving Maxwell's equations with specific boundary conditions that specify the physical characteristics of these obstructing objects. In an indoor environment, or in a ship setting, radio waves encounter multiple objects that vary in their properties and sizes. Such calculations are very hard to carry out because many parameters change from one object to another and are sometimes unavailable. Therefore, approximations have been developed to characterize signal propagation without resorting to a direct solution of Maxwell's equations. The most common approximations use ray tracing techniques, as well as analytical and statistical models. Chapter III of this thesis discusses some of the indoor propagation models and introduces the Urbana code.

III. INDOOR PROPAGATION

As illustrated in the previous chapter, propagation in an indoor environment is governed by two principal mechanisms: (1) attenuation due to walls and obstacles, and (2) scattering (reflection and diffraction from obstructions). Because indoor environments vary widely in the materials used for the different walls, doors, and windows, and because of the variable size, number, and geometrical layout of the rooms, it is hard to find a generic model that can accurately model a very specific indoor setting. This chapter introduces three model types (free space model, empirical models, and physical models) that characterize signal propagation in an indoor environment.

The chapter also shows the advantages and disadvantages of each model and explains where the Urbana code falls as a modeling tool. Later chapters describe the specific characteristics of Urbana.

A. FREE SPACE PATH LOSS MODEL

The simplest model to account for losses between a transmitter and a receiver is known as the free space path loss model. The loss between the end points of a link is nothing but the difference between the power input at the receiver P_r and the power output at the emitter P_t. In this case, it is assumed that there are no obstructions between the transmitter and the receiver and that the signal propagates along a straight line of sight (LOS) between the two. Starting from the Friis transmission equation [7],

$$P_r = \frac{P_t G_t G_r \lambda^2}{(4\pi)^2 d^2} \tag{23}$$

where G_t and G_r are, respectively, the transmitting and receiving antenna gains and d is the distance separating them. The free space path loss P_L between isotropic antennas is calculated as follows:

$$P_L \text{ [dB]} \equiv -\log\left(\frac{P_r}{P_t}\right)\Bigg|_{G_t=G_r} = -10\log\left(\frac{\lambda^2}{(4\pi)^2 d^2}\right). \tag{24}$$

It is important to note that the path loss is not a true loss of energy as in the case of the wave attenuation (as discussed in Chapter II). This loss always occurs even if the medium itself is lossless. It is mainly due to the fact that the energy carried by the spherical wave is flowing in directions other than towards the receiver.

In a ship environment, things are more challenging. Although the free space path loss will always occur, many other sources of energy loss must be considered. For example, in a compartment crowded with shipboard equipment, propagation mechanisms become more complex and many reflections and diffractions take place. The details of the environment change from one compartment to another, and even varying the antenna location or opening a door within the same compartment might greatly affect the signal distribution.

To account for these, a number of more sophisticated models have been developed to make it easier to predict the way waves behave in an indoor environment. These models can generally be classified as either empirical or physical.

B. EMPIRICAL MODELS

Empirical models (also called statistical models) are based on fitting curves or analytical expressions to observed data, such that the propagation mechanisms are accounted for in an average sense [9]. Often, these models lead to satisfactory results for a collection of indoor environments with similar characteristics to the ones where the actual measurements were taken. In addition, they are simple, fast (do not necessitate a lot of computations), and do not require a detailed knowledge of the environment where the waves propagate.

Nevertheless, these models do not provide reliable results when applied to complicated indoor environments such those found on shipboard compartments, and cannot be universally used. They do not take advantage of possible prior knowledge of the physical environment, are not constrained by the laws of physics, and always require some sort of measurements to be curve-fitted in order to extract a usable expression.

Although many empirical models for urban and outdoor propagation exist, such as the European Research Committee COST 231 model and the HATA models [10], only a few empirical models were developed for indoor applications. The Honcharenko and Bertoni models [11, 12] are examples of empirical indoor propagation models.

A comparison between the results of an empirical model and those of measured data is shown in Figure 12 from Ref. 13. The results show the variation of the received signal strength in an underground street that contains shops with a high density of pedestrians. The results are presented for daytime, night-time and vertically and horizontally polarized antennas at the 10-GHz, 5.5-GHz and 800-MHz frequency bands. Based on the measured data, the only derived statistical parameter is the attenuation constant (expressed in dB per 100 m in the figure).

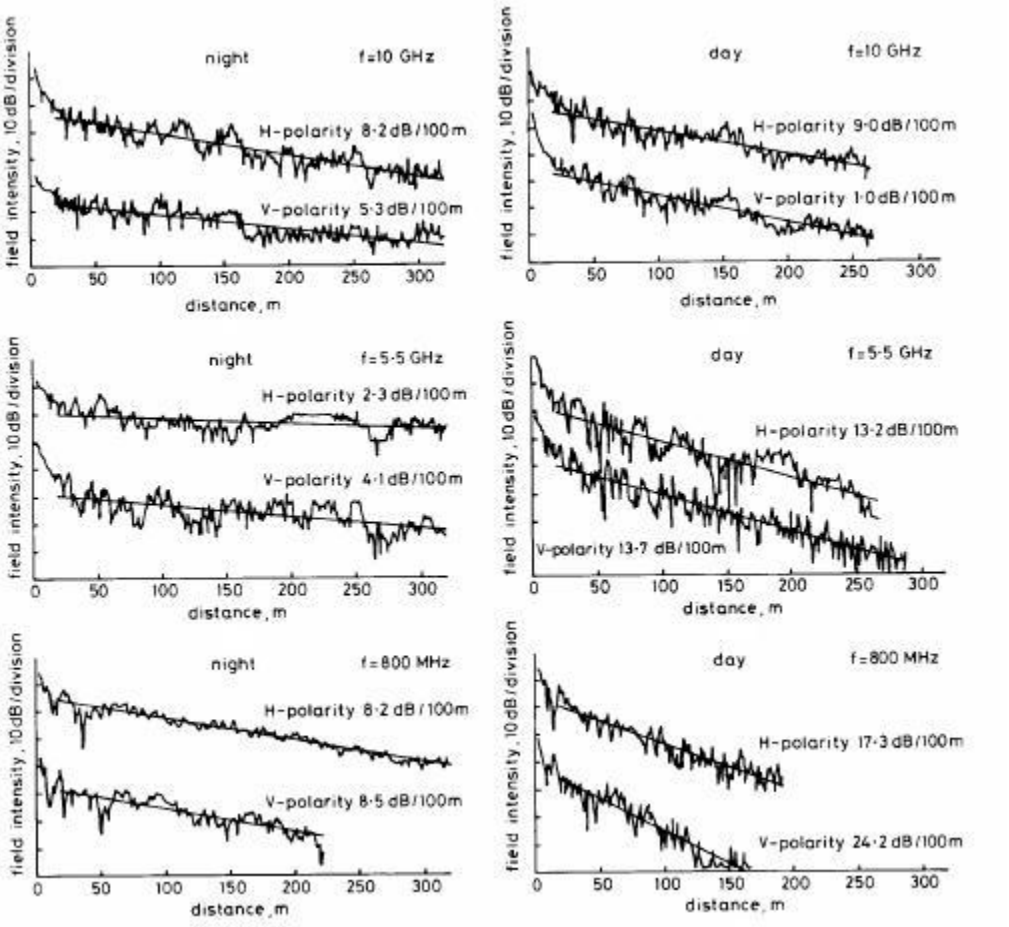

Figure 12. Received field strength along an underground street [From Ref. 13.]

C. PHYSICAL MODELS

Physical models, also called deterministic or site specific (SISP) models, take into account the specific characteristics (geometry, materials, location, size, etc.) of the different elements that make up the indoor environment being modeled. With the continuing growth of computing power, these models have become more appealing to predict indoor propagation. They use various ray tracing techniques and largely depend on the electromagnetic laws of physics to predict the signal level based on the precise details of the environment (rooms, ship compartments, office buildings, etc.).

Site-specific models take advantage of the high-frequency approximation permitted when the primary scattering objects like walls and furniture are large compared to the wavelength, which enables the simulation of radio frequency propagation in terms of rays. This approximation is obviously valid for the 2.4-GHz band where the wavelength is 0.125 m. Therefore, the resulting field strength at any given receiver location is computed as the sum of all contributing rays arriving at that location from the transmitter. These codes are capable of modeling high-order propagation mechanisms such as multipath and diffraction, which allows signals to be received behind walls and in shadow areas that do not have a line-of-sight path.

Although physical models lead to more accurate results and do not depend upon prior measurements, these models tend to be computationally demanding in memory and CPU time and, practically speaking, cannot be used to model every possible scenario for a problem.

Urbana is a physical model because it takes into account the geometry of the environment at hand, accepts material properties of the different constituents of the geometry, and uses a ray-tracing engine (coupled with proprietary algorithms to implement physical optics (PO), geometric optics (GO), and diffraction physics) in producing a 3-D simulation. Chapter IV gives an overview of the Urbana code and its characteristics.

IV. URBANA SOFTWARE OVERVIEW

Previous chapters explained the fundamentals of wireless propagation and introduced some of the models that can be used to simulate EM propagation in an indoor setting. This chapter gives an overview of the Urbana software that was used for the simulation part of this research. In particular, this chapter examines the major components of the software and guides the reader through the different steps in generating the Urbana input file, running the code, and post-processing the results. The last part of the chapter talks about some of the benefits of the Urbana code as compared to other propagation models.

A. INTRODUCTION TO URBANA

Urbana is a computational electromagnetic tool for simulating wireless propagation and near-field radar sensors in complex environments. Users of the code can assess antenna, network and radar system designs in a wide range of settings such as outdoor, urban, rural, and indoor environments.

The software's ray tracing engine can account for intricate and multi-bounce effects introduced by multiple walls, obstacles, and many other penetrable obstructions. To simulate electromagnetic wave propagation in urban environments, Urbana uses 3-D ray tracing applied to 3-D models of terrain, buildings and other features [14].

The software can be used to [14]

- Predict area field coverage, as well as fading and co-channel interference.
- Conduct parametric antenna pattern and polarization studies.
- Predict multiple propagation paths that are distinguished according to signal strength, angle of arrival and delay.
- Present comparative studies for base station placement.
- Identify multi-path and diffraction propagation mechanisms.

The key inputs to the Urbana code (as they appear in the input file) are:

- Facet model for terrain, buildings, and other features.
- Placement, power output, and polarization of the antenna.
- Plane of observation points.

- Edge model for terrain, buildings and other features (can be extracted from the facet model in the Cifer application described below).
- Propagation computation model.
- The different surface material properties (PEC, concrete, glass, dielectrics, etc.)

The key outputs are:

- Composite field level at each observation point.
- Angle of arrival, polarized strength, and delay of each arriving signal.

B. MAJOR COMPONENTS OF THE URBANA CODE

The Urbana software is made of a suite of programs that are executed in modular sections. A brief description of each program and the relationships within the suite of programs is discussed next.

1. Geometry Builder

Although ACAD is the default geometry builder for the Urbana code, it is not widely distributed and supported. The Rhino design software was used to generate building structures and geometries for this project. In addition to having all the required capabilities, Rhino has proven to be widely available and easier to learn. Chapter V gives more details on the Rhino software.

2. Cifer

Cifer has two major sets of commands. The “convert commands” are used to translate building files imported from other drawing programs (CAD, IGES, BRL, etc.) and to write them into the “.facet” file format required by Urbana. The “edit facet” set of commands is capable of:

- Cleaning and compressing facet files.
- Executing edge extraction.
- Rotating, translating, scaling and clipping.

- Creating ground planes.
- Manipulating material and component operations.
- Combining multiple facet/edge files.
- Creating simple geometric shapes (boxes, cylinders, cones, etc.)
- Adding or changing simple geometric shapes (boxes, cylinders, etc.)

3. Xcell

Xcell is the primarily visualization tool used to interactively view and modify the structure and environment models that are input to Urbana. More specifically, the user builds the complicated environment (geometry) and then checks its correct arrangement with Xcell. This application can also be used to remove facets or edges and to change the material properties and assignments for the facets of a specific geometry.

4. Plane-of-Observation Points Builder

The Obvpoint.m Matlab code in the Appendix generates an observation plane that can be added to the geometry file. The program asks the user to input the boundary values of the *x*, *y*, and *z* coordinates of the observation plane as well as the needed step size (resolution). It then returns an ASCII file with a list of observation points that can be read by the Urbana input file.

C. RUNNING URBANA INPUT FILE

Urbana is the computational engine that determines the signal level for the specified inputs (frequency, antenna types, building geometry, etc.). There are several electromagnetic algorithms to select from, but all are based on a high frequency assumption. Upon execution, Urbana reads an input file that has an ".ur_input" extension. It is an ASCII file that is comprised of a series of code words followed by the computation parameters. A sample input file is included in Appendix. There are comment lines describing the parameters and their range of values, so modifying the file is relatively straightforward.

The input requires a geometry file that must have a ".facet" extension. Urbana requires a triangular facet model (also called a mesh model) of the surfaces. Clearly complex surfaces, including curved ones, can be represented by triangles to any accuracy desired by making the triangles as small as necessary. In addition, the input code requires an ".edge" file to account for all the edges in the ".facet" geometry model. All of the antenna parameters (type, location, and power output) can be either input directly into the code or specified in an ".antenna" file that Urbana can read. The last data input file required by the code is the observation points file. This is the ASCII file that the obvpoint.m Matlab file returns when it generates the plane of observation points.

Once the input file is ready, the program's calculation engine is launched. At the end of each simulation, an output file with an extension ".field" is created. A summary of the different steps in generating the Urbana input file and running Urbana is shown in the Figure 13.

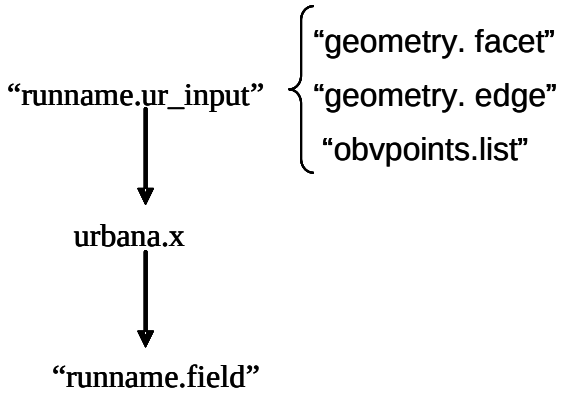

Figure 13. Components of an Urbana input file and running Urbana

D. POST PROCESSING URBANA OUTPUT FILE

The "runname.field" generated in the previous step is then converted into a ".facet" file by using the f2f command in Urbana. Once in a ".facet" format, the final results of the signal spread can be viewed in Xcell. When going from the ".field" format to the ".facet" format, the user selects the magnitude of the electric field to be displayed (E_x, E_y, E_z, or E_{total}), the dynamic range to be used (based on the calculated minimum and maximum signal levels recorded), the antenna power level scale factor, the number

of color levels to represent the chosen dynamic range, and the position of the observation plane with respect to the original geometry. Figure 14 summarizes the different steps in post processing the Urbana results.

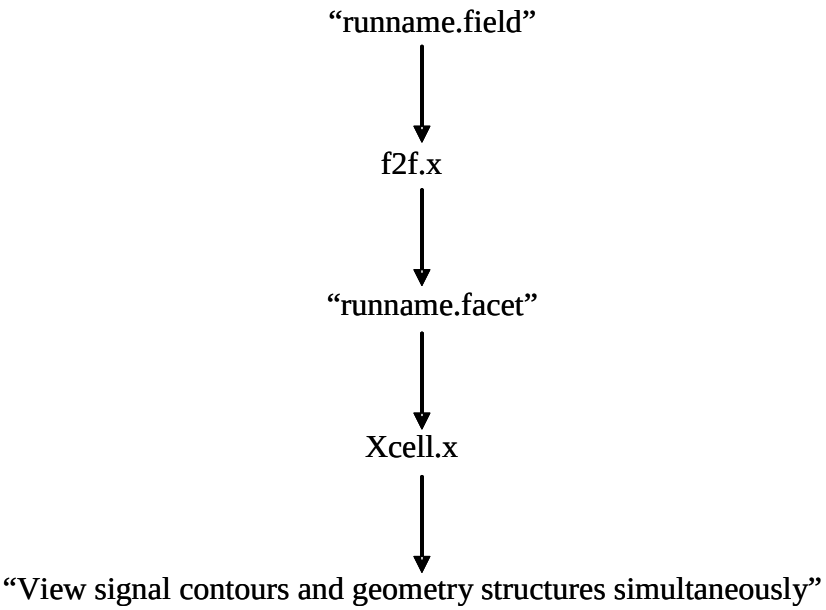

Figure 14. Post processing Urbana results

Figure 15 shows an example of a ".facet" file displayed in Xcell, where the user can see signal contours and geometry structures simultaneously. This is the final product for most simulations conducted in this thesis. The structure edges are displayed as black lines.

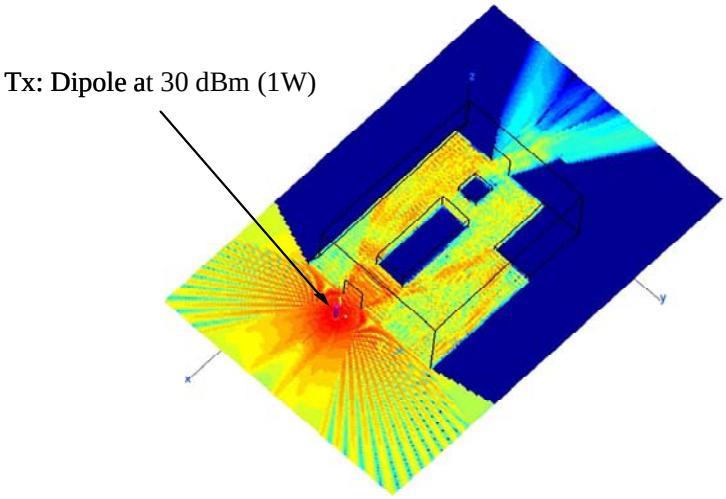

Figure 15. Example of Urbana output results

A color bar composed of 25 colors between blue and red, representing the variation in signal strength level between the minimum and maximum of the dynamic range chosen. It is added to each simulation result to help better interpret the signal spread. Figure 16 shows the color bar that is used for all simulations in this thesis.

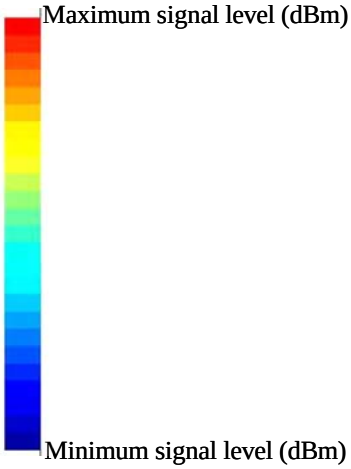

Figure 16. Color bar

E. BENEFITS OF THE URBANA CODE

As seen in Chapter III, indoor propagation analysts are frequently confronted with a complex environment that is difficult to characterize with simple formulas. This leaves them with two options: 1) on site measurement and 2) propagation analysis tools. While measurements are always an available solution, they are expensive, time consuming, and do not provide any insight into physical causes. They do not always allow broad generalization nor lend themselves to "what if" scenarios. Urbana's capability to analyze multiple “what if” scenarios makes it a great tool for the simulation and comparison of different systems in a variety of environments [15]. In addition, Urbana can use models of structures that include details such as doorways, wall thickness, and associated material properties, to accurately characterize the building structure, and thus return more precise results.

As discussed in this chapter, the first step in running a simulation is the development of a geometry model of the environment to be simulated. Chapter V presents some of the naval ship compartments that were developed for the purpose of this thesis.

V. DEVELOPMENT OF TYPICAL SHIPBOARD COMPARTMENTS

The previous chapter stated that a geometry file is necessary to run the Urbana code. This chapter continues the discussion by providing an overview of the Rhino software that was used to generate the geometry models for this thesis. The chapter also provides details of the models of shipboard compartments (missile room, combat information center, bridge, and study area) that are used in Chapter VII.

A. OVERVIEW OF THE RHINO SOFTWARE

Most of the geometry models for the ship compartments used in this thesis were built with the Rhinoceros Version 2.0 software. Rhino is an uninhibited free-form, 3-D, Non-Uniform Rational B-Spline (NURBS), modeling tool that can model arbitrary shapes. The decision to use Rhino, rather than the default CAD software (ACAD) that is usually used with Urbana, is based on the following criteria [16]:

- Rhino provides the necessary tools to accurately model, render, animate, prototype, analyze, draft, and build any 3-D model.
- Models built in Rhino can be written in an ".iges" format, and then read in a ".facet" format using the Cifer application in Urbana.
- Rhino runs on a laptop or an ordinary Windows PC.
- Rhino is straightforward to use and makes it possible to focus on design and visualization without being distracted by the software itself.
- Rhino enables the user to capture a physical model onto the computer.
- Rhino is fast, even on an ordinary laptop computer. No special hardware is needed.
- Rhino is also affordable. It is priced like other Windows software and requires no maintenance fees.
- Rhino is compatible with almost all other design, drafting, engineering, analysis, rendering, animation, and illustration software.
- Support and training for Rhino is available in the Total Ship Systems Engineering (TSSE) lab in Bullard Hall at the Naval Postgraduate School, Monterey, CA.

B. DETAILS OF THE RHINO SOFTWARE

As illustrated by Figure 17, the default Rhino editor layout contains four view ports configured as the top, front, right, and perspective view. Each view port can also be stretched to fill all or any portion of the screen. Like most 3-D modeling applications, object creation is done on construction planes.

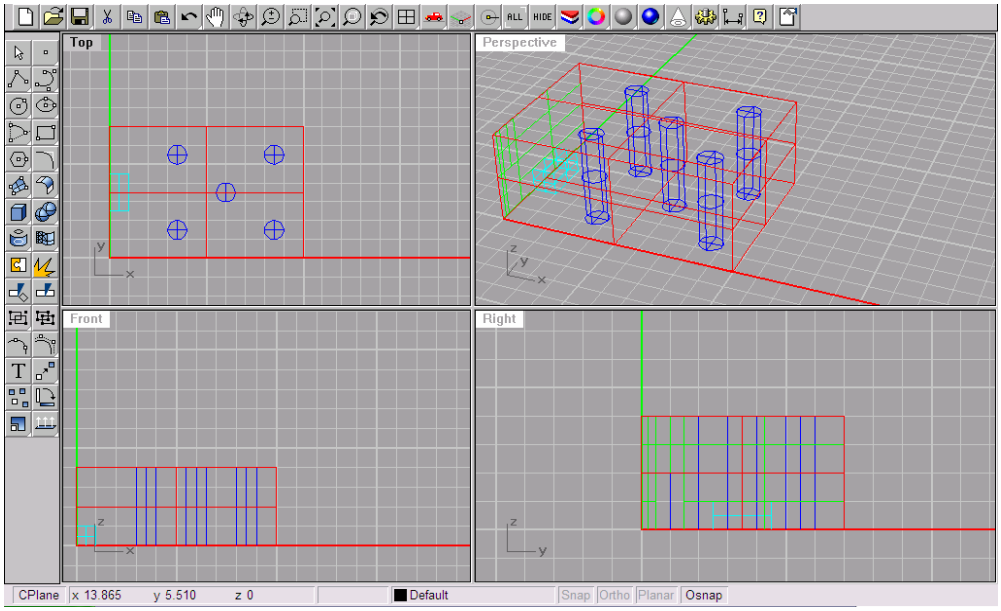

Figure 17. A snapshot of a Rhino editor layout

Another interesting aspect of object creation in Rhino is the ability to complete commands initiated in one view in another one. The cursor is active in all view ports. This provides good 3-D feedback while creating elements of the model.

The coordinate system origin defaults to the center of each view port. Rhino export honors the coordinate system origin used to create the model. Thus, it comes into the Xcell window in proper relation to the current model. This is taken into account during construction of the models of shipboard compartments for this thesis.

Rhino models are exported in ".iges" format and then imported in ".facet" format by using the Cifer application in Urbana.

Rhino runs on ordinary Windows desktops and laptop computers with the following requirements [16]:

- Pentium, Celeron, or higher processor.
- Windows 98/NT/ME/2000/XP for Intel or AMD.
- 65 MB disk space.
- 128 MB RAM.
- Open GL graphic card recommended.
- IntelliMouse recommended.

C. SAMPLE EXAMPLES OF SHIPBOARD COMPARTMENTS

The goal of this thesis was to assess the performance of a WLAN in typical naval compartments. Because naval compartments vary by ship type, size, and mission, a wide range of compartments, from a missile room of a fast patrol boat to a library of an aircraft carrier, were developed. Although the geometries reflect some existing compartments, their dimensions are only approximate and do not represent real dimensions measured on board any of the U.S. or foreign Navy ships.

1. Missile Room

Figure 18 represents a typical missile room compartment of a naval vessel. This compartment was developed using both the Rhino software and the Cifer application. First, the whole compartment was built using Rhino. After going through the translation process from ".iges" format to ".facet" format, the cylinders were distorted and could not be clearly viewed in Xcell. Several fixes were tried to solve this problem. These included increasing the tolerance used in Rhino, and the discretization displacement error tolerance in Cifer. Because none of the fixes were successful, it was decided not to build any circular shapes using Rhino, but rather add them later in Cifer. The missiles were built in Cifer while the rest of the compartment was built using Rhino. Then, they were combined using the "combine option" in Cifer.

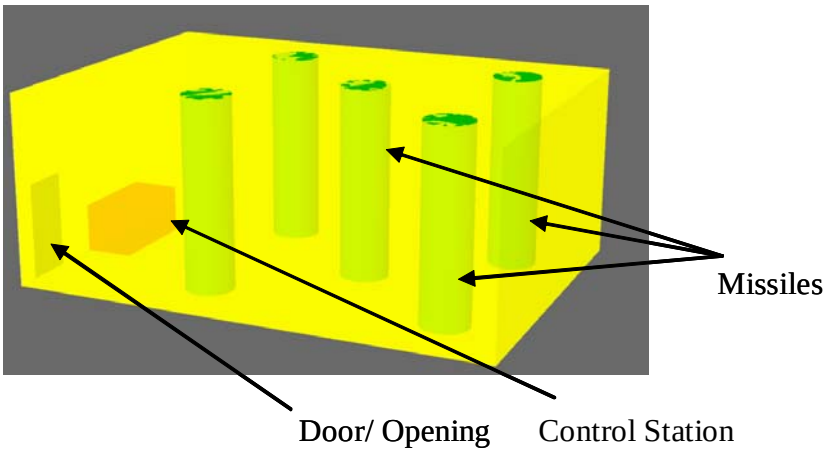

Figure 18. Missile room compartment

Figure 19 gives more detail on the dimensions of the missile room shown in Figure 18. All dimensions in this thesis are in meters.

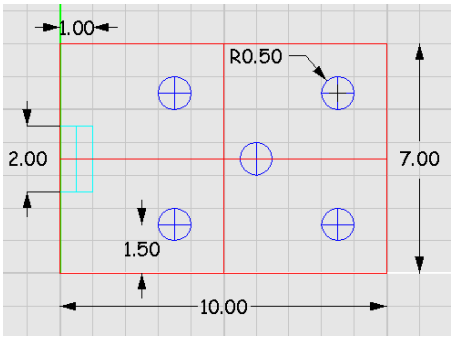

Figure 19. Missile room dimensions (m)

2. Combat Information Center

The second compartment developed was a typical Combat Information Center (CIC) on a fast patrol boat. The whole compartment was developed using Rhino. There were no problems transferring it from ".iges" format to ".facet" format through Cifer. This compartment has two doors and one hatch in the ceiling. All doors are drawn open in Figure 20 but can be easily closed for simulation purposes. That can be done by overlapping a surface that has the same dimensions over the opening, and then doing a consolidate check in Cifer to make sure that all edges are consolidated. The "consolidate check" step is imperative to prevent problems with edge diffractions due to multiple edges present at the same edge location.

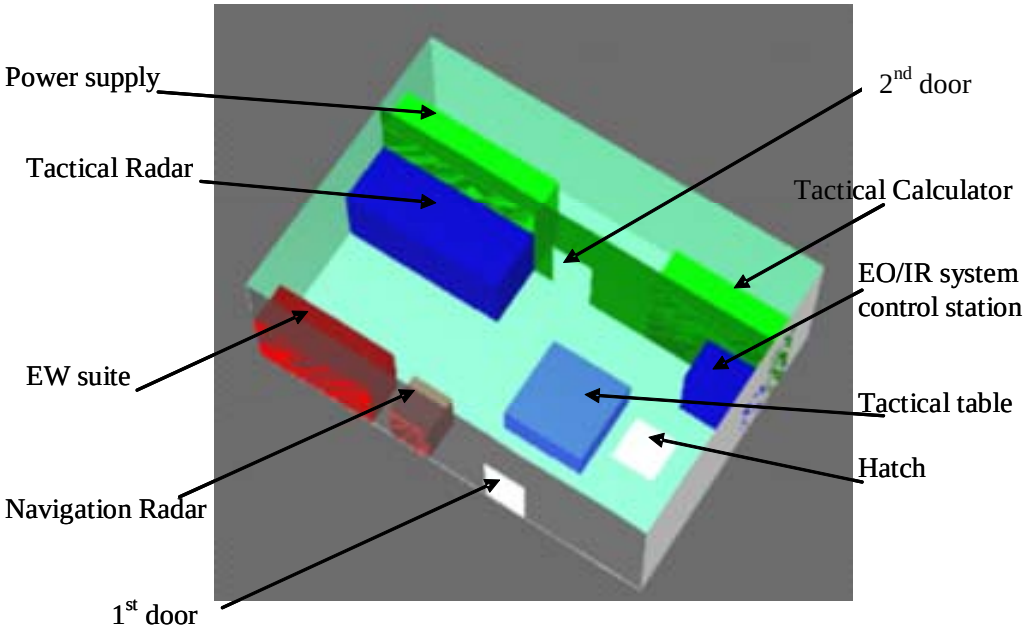

Figure 20. CIC compartment

Figure 21 illustrates the actual dimensions of the CIC compartment shown in Figure 20.

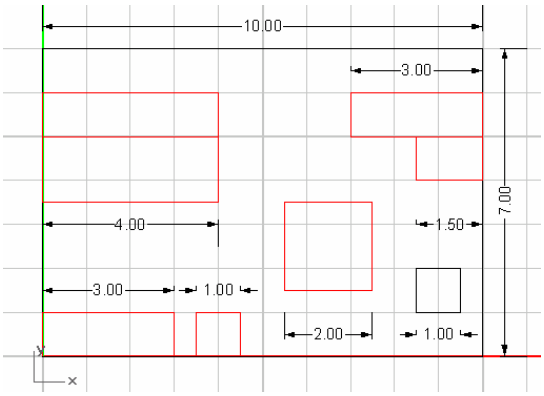

Figure 21. CIC Dimensions (m)

3. Bridge

A simple model of a bridge on a fast patrol boat is shown in Figure 22. It consists of a machinery control unit, navigation radar, and chart table. This bridge has two doors (port and starboard). There is also a hatch that allows access to lower levels. The front bulkhead of the bridge contains the viewing windows.

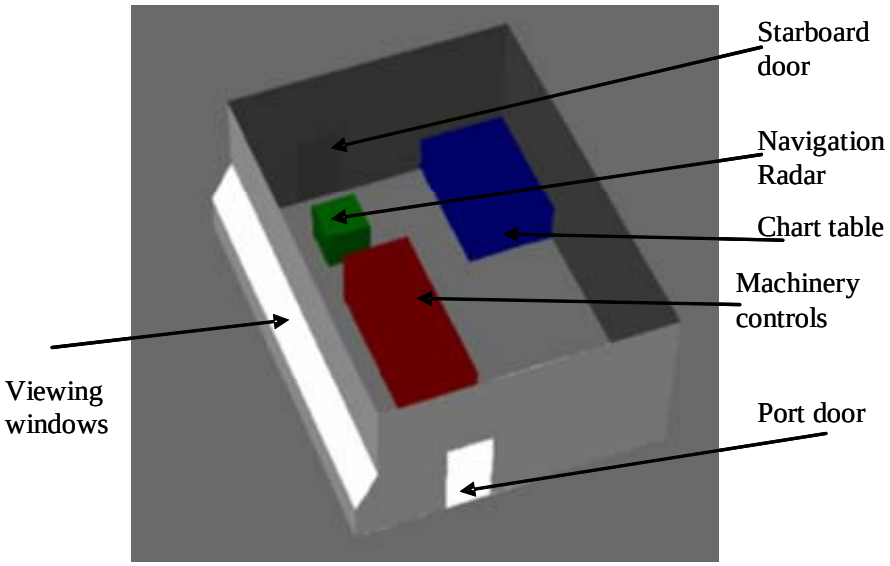

Figure 22. Bridge compartment

Because Urbana recognizes materials based on their ICOAT number, the windows were assigned a different ICOAT number than the rest of the compartment. The ICOAT number of the windows represented the material properties of glass. The rest of the compartment had an ICOAT=0, to signify the material properties of a perfect electric conductor (PEC).

Because of the need to assign dissimilar ICOAT numbers for different surfaces of this compartment, all surfaces of the same ICOAT number were built at one time, but as separate surfaces from others that do not share the same ICOAT number. Each group of surfaces that have the same ICOAT number is then translated from an ".iges" format to a ".facet" format and assigned a specific ICOAT number that reflects its material properties. Finally, all surfaces are assembled together using the "consolidate facet files" option in Cifer, and saved as a single ".facet" geometry to be read by Xcell.

At the conclusion of the consolidation step, objects with unlike material properties preserved their ICOAT numbers. Each ICOAT number is then defined in the Urbana input file to represent a specific material.

Figure 23 gives more details on the dimensions of the different elements of the bridge.

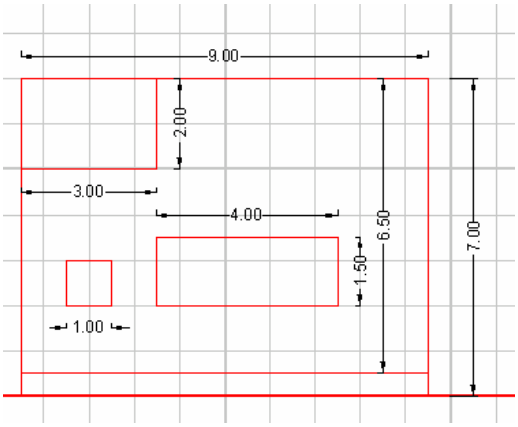

Figure 23. Bridge dimensions (m)

4. Study Area

Another compartment developed was an example of a study area that could be found onboard a large naval vessel. The walls, study spaces, and cubicles were developed separately to allow for material selection before all pieces of the geometry are grouped. The outer walls are made of a PEC material. Depending on the simulation objective, the inner wall material properties varied between PEC, wood and composite.

This compartment has two openings (front door and back door) but no hatches for upper level or lower level access. Each study space has a door opening that makes it a closed space when the door is added. The cubicles have only sidewalls and a back wall as is shown in Figure 24. Figure 25 shows the dimensions of the proposed study area that was simulated.

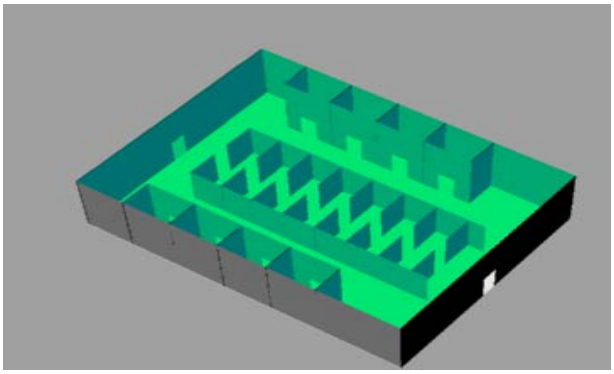

Figure 24. Study area compartment

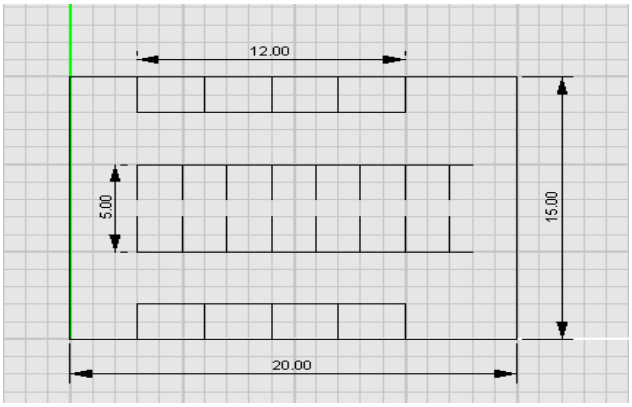

Figure 25. Study area dimensions (m)

5. Combination of Compartments

During the simulation part of this research, it was deemed necessary to study the propagation of waves between same floor compartments. The CIC and missile room compartments were combined to create two adjacent compartments and to study how waves propagate through openings from one compartment to the other. Figure 26 shows what is referred to as the “CIC_MissileRoom” compartment.

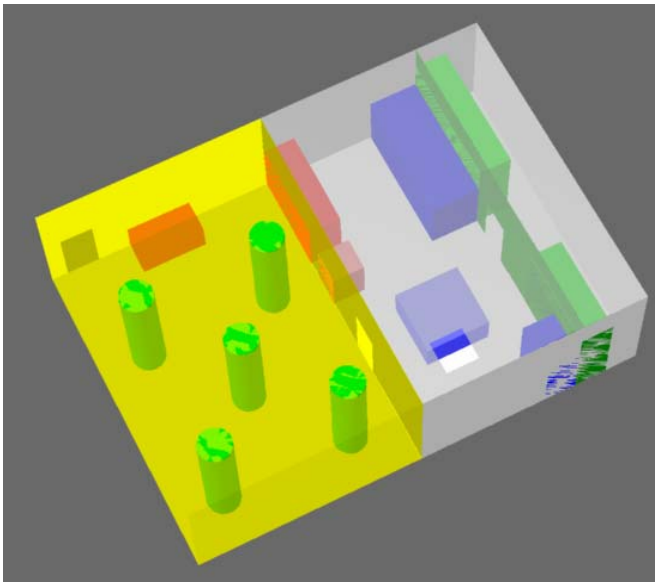

Figure 26. CIC_MissileRoom compartment

Also, it is important to note that, before the two geometries were consolidated, it was necessary to delete the right side wall of the missile room. That was easily done in Xcell by selecting all the facets in the wall and deleting them. This action was necessary

because, in reality, only one wall joins the two compartments. A second full wall from the missile room side would have blocked the CIC door and made it look as if there was no opening there.

After generating the different geometry models to be used for the simulation part of this thesis, the subsequent step in running the Urbana code is the selection of the different input file parameters. Chapter VI presents possible choices for each of the input parameters and conducts a careful examination, and selection of these parameters.

THIS PAGE INTENTIONALLY LEFT BLANK

VI. SELECTION OF INPUT FILE PARAMETERS

As discussed in previous chapters, in addition to the input data files, the antenna file, and the observation points file, Urbana requires the user to select a variety of parameters that define vital options on how Urbana runs the simulation. This chapter conducts a careful examination of the different computation methods available, possible antenna patterns and polarizations, material properties that can be used, frequency bands available, possible number of ray bounces, and finally possible ray launch angles.

Some simple geometrical examples are included to assess the performance of the Urbana code as the input parameters are varied. Based on the results of the assessment conducted in this chapter, a selection of the major input parameters that are used in the simulation part of this research is made.

A. PROPAGATION COMPUTATION METHOD

The Urbana code offers three computation methods. The fields can be computed in the absence of a scatterer, or by either the geometrical optics (GO) or the shooting and bouncing ray (SBR) methods. To account for edge diffraction, the SBR and GO computation methods can be enhanced by either the physical theory of diffraction (PTD) or the geometrical theory of diffraction (GTD), respectively.

All simulations in this thesis are based on the GO computation method. This is done by selecting "2" in the Urbana input file as is shown in Figure 27.

```
#--- Choose method of computation
#    0 = compute fields in the ABSENCE of the scatterer
#    1 = compute fields by SBR
#    2 = compute fields by GO
2
```

Figure 27. Selection of the GO computation method

This section examines whether the enhancement of the GO computation method with the GTD is necessary. In order to serve that purpose, a simple corner edge diffractor model, as shown in Figures 28, was developed.

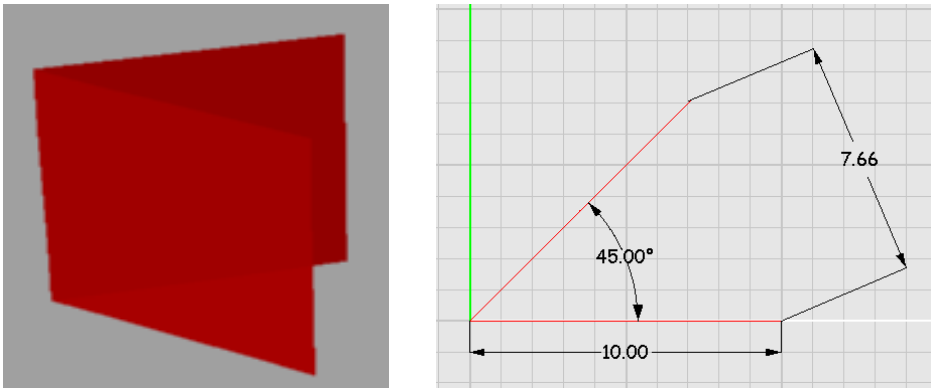

Figure 28. Corner edge diffractor

1. Case 1: Simulation with No Edge Diffraction

This simulation was run with GO only, so that edge diffractions are not included. The simulation parameters are listed in Table 2.

Antenna location	(10 m, 5 m, 5 m)
Antenna type	1 W, $\lambda/2$ dipole
Antenna polarization	Vertical
Observation points plane	x = (–10 m, 15 m); y = (–5 m, 15 m); z = 5 m
Frequency	2.4 GHz
Computation Method	GO
Edge diffraction	No edge diffraction
Material properties	All PEC
Dynamic range	90 dB

Table 2. Corner edge simulation with no edge diffraction

Because the edge diffractor walls are made of a PEC material, there is no direct propagation through the walls. The wall edges appear as black lines. As is shown in Figure 29, all emitted waves are reflected when they hit the reflector surface. This explains the varying signal strength at the observation points inside the area delimited by the corners of the edge diffractor surfaces.

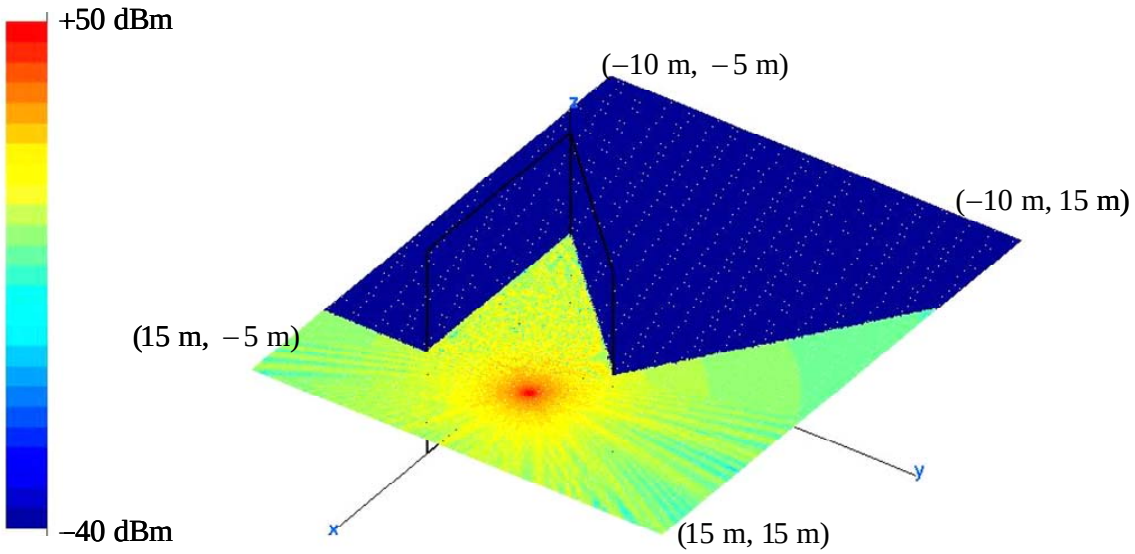

Figure 29. Case 1: corner edge simulation with no edge diffraction

The simulation results clearly show that there is no edge diffraction because there is no field in the shadow regions. The signal strength starts high and decreases as we move away from the antenna source (purely a consequence of inverse square law of the path loss). Depending on the locations of each of the observation points, they experience some sort of interference between the direct rays and reflected rays and, hence, the variable signal strength of observations points located at the same radial distance from the source.

The blue color indicates signal strength that is equal to or below -40 dBm. The red color indicates signal strength values that are equal to or exceed $+50$ dBm.

2. Case 2: Simulation with Edge Diffraction Added

In this case, GO is enhanced with GTD and everything else is kept the same. The results, as shown in Figure 30, clearly show the effect of including edge diffraction. Higher signal strengths are noticed behind the corner edge surfaces because waves are diffracted at the edges. The primary result that can be deduced from this simulation is that when using the Urbana code, it is essential to account for the edge diffraction phenomena. As a matter of fact, edge diffraction can be the primary propagation mechanism in the case of indoor propagation, where many shadow areas can be found.

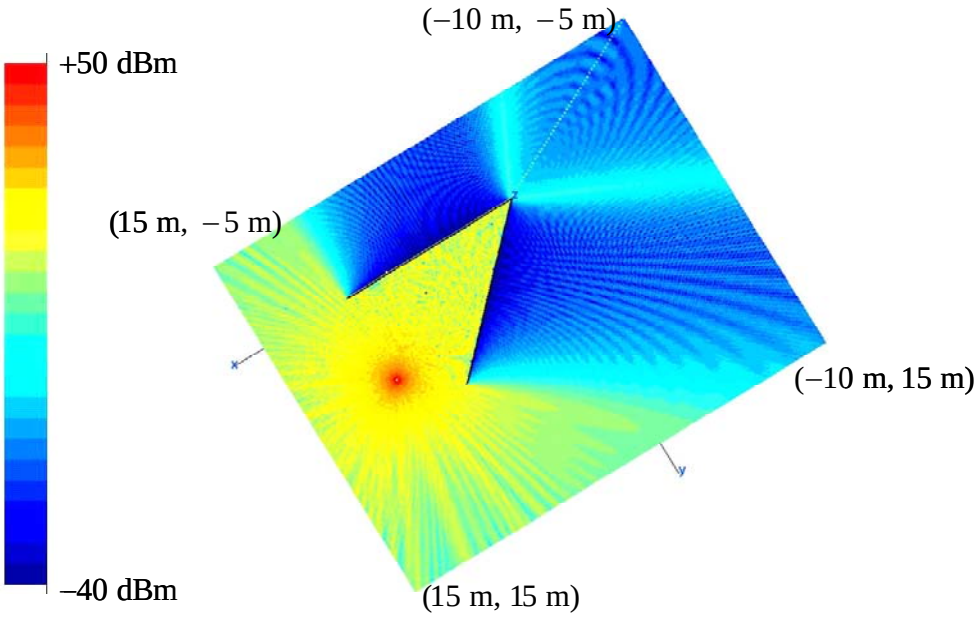

Figure 30. Case 2: corner edge simulation with edge diffraction

3. Case 3: New Antenna Location with No Edge Diffraction

In this simulation, the same input parameters as case 1, except for the antenna location, are used. This is done to prove that the results drawn from case 1 are independent of the antenna location. Again, no edge diffraction is added and the new antenna location is (–5 m, –2.5 m, 5 m). The results of this simulation are shown in Figure 31.

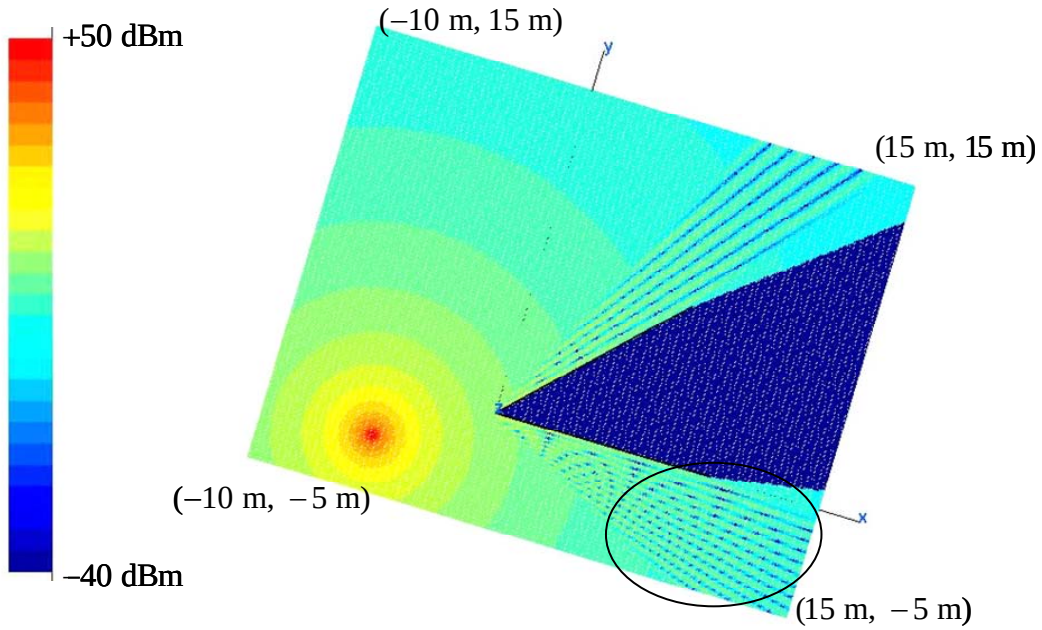

Figure 31. Case 3: corner edge with no edge diffraction

It is clear that waves are not diffracted at the edges and therefore no waves are present in the interior region of the corner edge diffractor. An obvious drawback of using only simple GO techniques to predict field strength includes the inability to predict field strength in shadow regions. Signal strength starts high (red color) and decreases in a $1/r^2$ fashion, where r is the radial distance from the source. Due to multipath, observation points in the circled region experience a fluctuating signal strength.

4. Case 4: New Antenna Location with Edge Diffraction

The result of the simulation when GO is supplemented by GTD is shown in Figure 32. Just as it was concluded for case 2, edge diffraction permits waves to propagate into shadows and significantly increases the signal strength at locations that had no signal present when edge diffraction was not included. The area right behind the corner (A) went from signal strength of less than -40 dBm in the no-diffraction case to about 0 dBm with edge diffraction present. Waves diffracted at the edges go through multiple reflections at the two surfaces of the corner edge and constructively add near the back corner to achieve significantly higher signal strength.

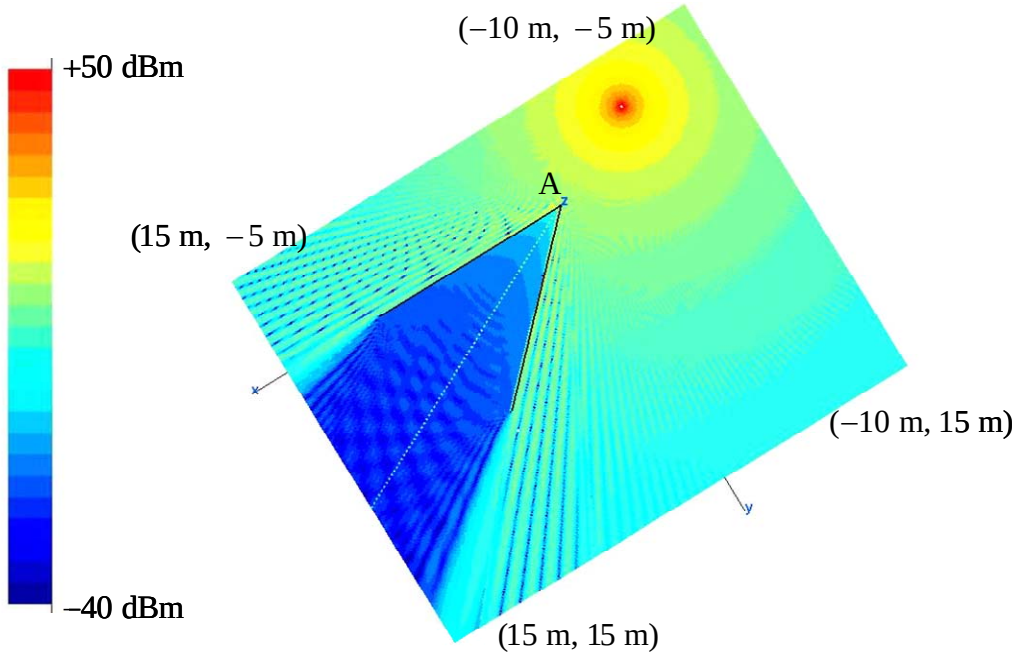

Figure 32. Case 4: corner edge with edge diffraction

Through the four previous cases, it was shown that the use of GO alone to simulate the behavior of waves is not precise enough. This becomes more apparent as the geometry of the compartment becomes more complex with many sources of diffraction. Because an accurate reading of the signal level must include all possible wave contributions, rays from GO and GTD must be combined to account for reflected-reflected, reflected-diffracted, and diffracted-reflected cases. Note that the diffracted-diffracted case is not included.

During the rest of the simulations in this thesis, the uniform theory of diffraction (UTD), which is an improved form of GTD, is used as an input to the Urbana input file as shown in Figure 33.

```
#--- Edge diffraction
#    SBR can be enhanced with PTD edge diffraction.
#    GO can be enhanced with GTD edge diffraction.
#    Add edge diffraction (0, 2=no, 1=ILDC (SBR or GO), 3=UTD (GO only)
```

Figure 33. Selection of UTD

B. SELECTION OF THE ANTENNA POLARIZATION

The polarization of waves is defined in terms of the time varying vector orientation of the electric field. Losses occur when the receive antenna polarizarion and the wave polarization are mismatched. In a ship environment, radio wave propagation involves multiple randomly disposed scatterers throughout the environment. The scattering tends to randomize any given polarization of the transmitted wave. Therefore, the choice of polarization for the transmitted wave is not a critical concern in an indoor wave propagation study. Lee and Yeh [18] presented measurements in a suburban environment that show that vertically polarized signals and horizontally polarized signals behave very similarly. Their local means are highly correlated and within ± 3 dB for nearly 90% of the time.

A study done by Chizhik, Ling, and Valenzuela [19] conducted for a single floor of a moderately complex office building (the partitions consist of sheetrock, concrete, glass and metal) found that, when both the receive and transmit antennas are vertically polarized, exact treatment of polarization gave essentially the same result as that obtained by assuming that the signals stay vertically polarized while undergoing reflections and transmissions through walls. Therefore, when considering propagation between vertically polarized antennas, depolarization loss may be ignored and prediction accuracy is not significantly affected by assuming that the field remains polarized in the vertical plane.

Because the WLAN antenna polarization is one of the system inputs that can be selected, it was decided to create a simple geometric model and investigate the results of varying the antenna polarization from vertical to horizontal. The model developed was the solid PEC prism shown in Figure 34.

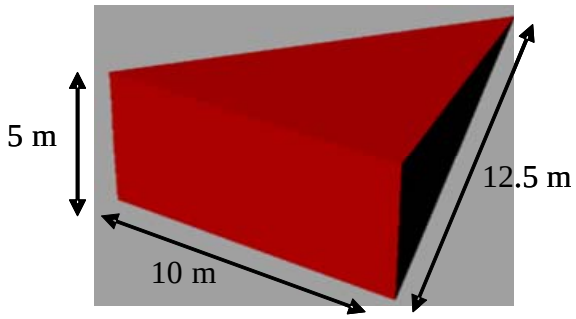

Figure 34. Prism geometry

The input parameters for the prism simulation are listed in Table 3.

Antenna location	(20 m, 5 m, 2.5 m)
Antenna type	1 W, $\lambda/2$ dipole
Antenna polarization	Vertical (case 1) ; horizontal (case 2)
Observation point plane	x = (−5 m, 25 m); y = (−5 m, 15 m); z = 2.5 m
Frequency	2.4 GHz
Propagation mechanism	GO with no edge diffraction
Material properties	All PEC
Dynamic range	90 dB

Table 3. Input parameters for the prism simulation

Figures 35 and 36 show the simulation results for the vertically polarized and horizontally polarized cases. It is clear from Figure 35 that the vertical antenna pattern is omni-directional.

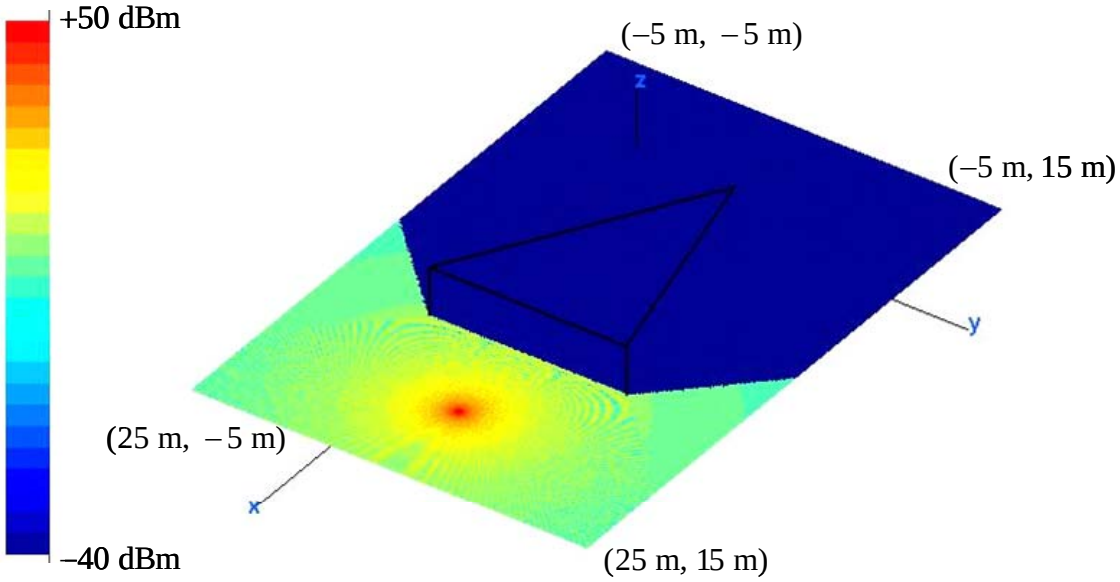

Figure 35. Vertically polarized antenna

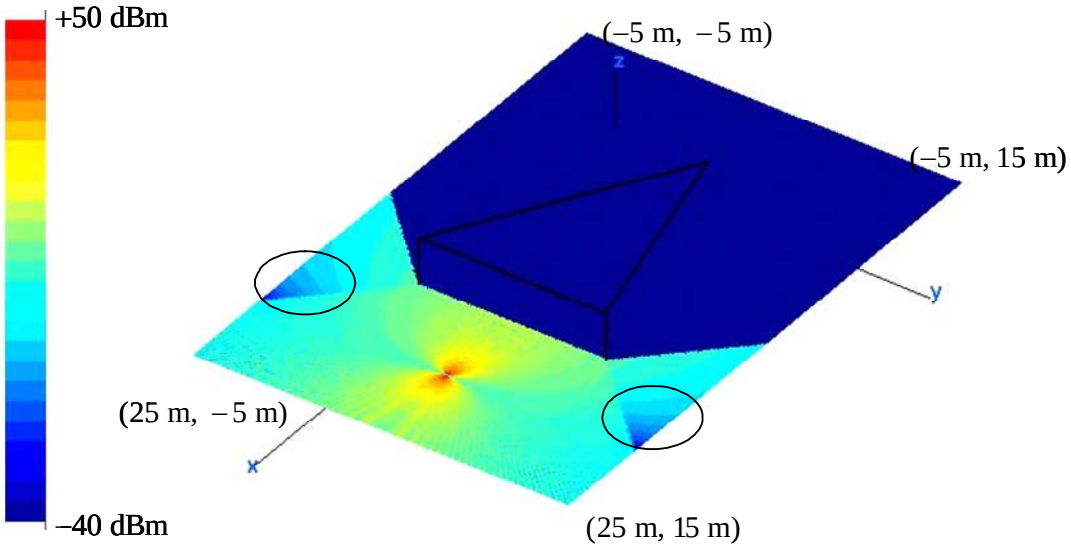

Figure 36. Horizontally polarized antenna

The circled areas on Figure 36 point to areas of significantly low signal level. This is due to the horizontal antenna pattern that points the antenna nulls in those regions and not to any specific propagation mechanism.

For this particular simulation, the vertically polarized antenna led to higher signal levels than the horizontally polarized antenna. Because most personal communication devices in use today operate with vertically polarized antennas to avoid the problem of nulls pointed at users, it was decided that measurements involving only vertically polarized fixed site antennas are presented in this research.

C. SELECTION OF THE ANTENNA PATTERN

In most cases, the signal spread in an indoor environment is a direct function of the radiation pattern of the antenna used. In every installation, the antennas should be made as directive as possible so as to only provide pattern coverage where needed. This should help to enhance signal strength as well as minimizing interference and multipath effects. Depending on the geometry at hand and the coverage area sought, one can make a decision on the antenna pattern to use.

Although a directional antenna is best suited for a point-to-point link (most apparent in outdoor propagation links), for most indoor links, many, if not all, installations require some omni-directional coverage that needs to be as uniform as possible. In order to accomplish the required omni-directionality, a vertical half-wave dipole antenna was used for most of the simulations in this research.

Because some of the commercial off-the-shelf (COTS) antennas that might be used with the WLAN have a directional behavior and because for some of the simulations in this research it was deemed necessary to use a directional antenna, a Matlab code that plots the pattern of a directional antenna was developed. The Matlab code is listed in Appendix. The user inputs the frequency and HPBW, and the code generates an ASCII pattern file that is saved for use by Urbana. Figure 37 shows a 15° -HPBW antenna pattern developed by the Matlab code and shown in Xcell. The observation plane is a cut through the antenna main beam. The antenna radiation pattern is zero in the rear hemisphere (behind the antenna).

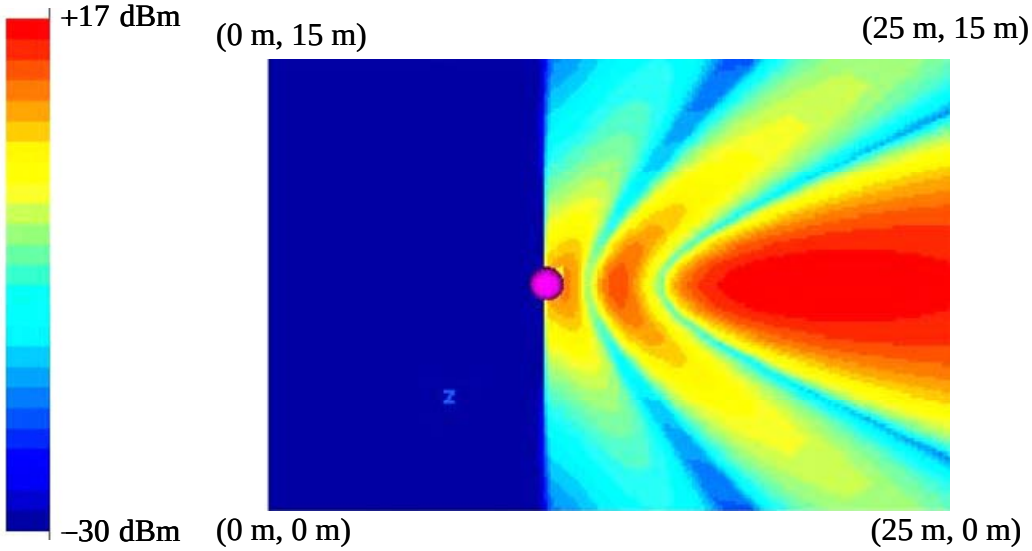

Figure 37. Directive antenna pattern

D. RAY LAUNCH AND BOUNCE OPTIONS

The Urbana code asks the user to input the following ray parameters: method of ray launch, ray density, angular interval between rays and maximum permissible ray bounces. Because GO is chosen as the computation method, only uniform angular distribution can be used as a method of ray launch (a requirement dictated by the code itself). In what follows, different options of angular intervals and permissible number of ray bounces are examined.

A simple geometry consisting of a rectangular room and a cylinder, as shown in Figure 39, was used for the purpose of this simulation. Different ray bounces have different colors.

Although Urbana allows the user to have angular intervals as low as 0.25 degrees and a maximum of 10 ray bounces, that usually leads to very long run times. Figure 39 summarizes the results of the simulation when the angular interval and number of ray bounces parameters were varied. Case (e) clearly shows that it is possible to have a full coverage of the compartment when the angular interval is two degrees and the maximum number of permissible ray bounces is five. Because most models of compartments used in this thesis have a comparable size to the compartment used in this simulation, the use of a two-degree launch angle interval and five maximum permissible ray bounces was deemed satisfactory. Figure 38 shows how these parameters are input into the Urbana input file.

```
#--- Choose method of ray launch
#    1 = by (baby) facet, achieving a uniform first bounce surface density
#    2 = uniform angular distribution (burst launch)
#    (If computation by GO, must select 2 = burst launch)
2
#--- If ray launch by (baby) facet (1 above), enter ray density:
#    # rays/wavelength (normally 5-10)
5.
#--- If burst ray launch (2 above), enter angular interval (deg).
#    (Typically 0.25 - 2.0 deg)
2.
#--- max permissible ray bounces (normally 5-10)
5
```

Figure 38. Selection of angular launch interval and maximum number of ray bounces

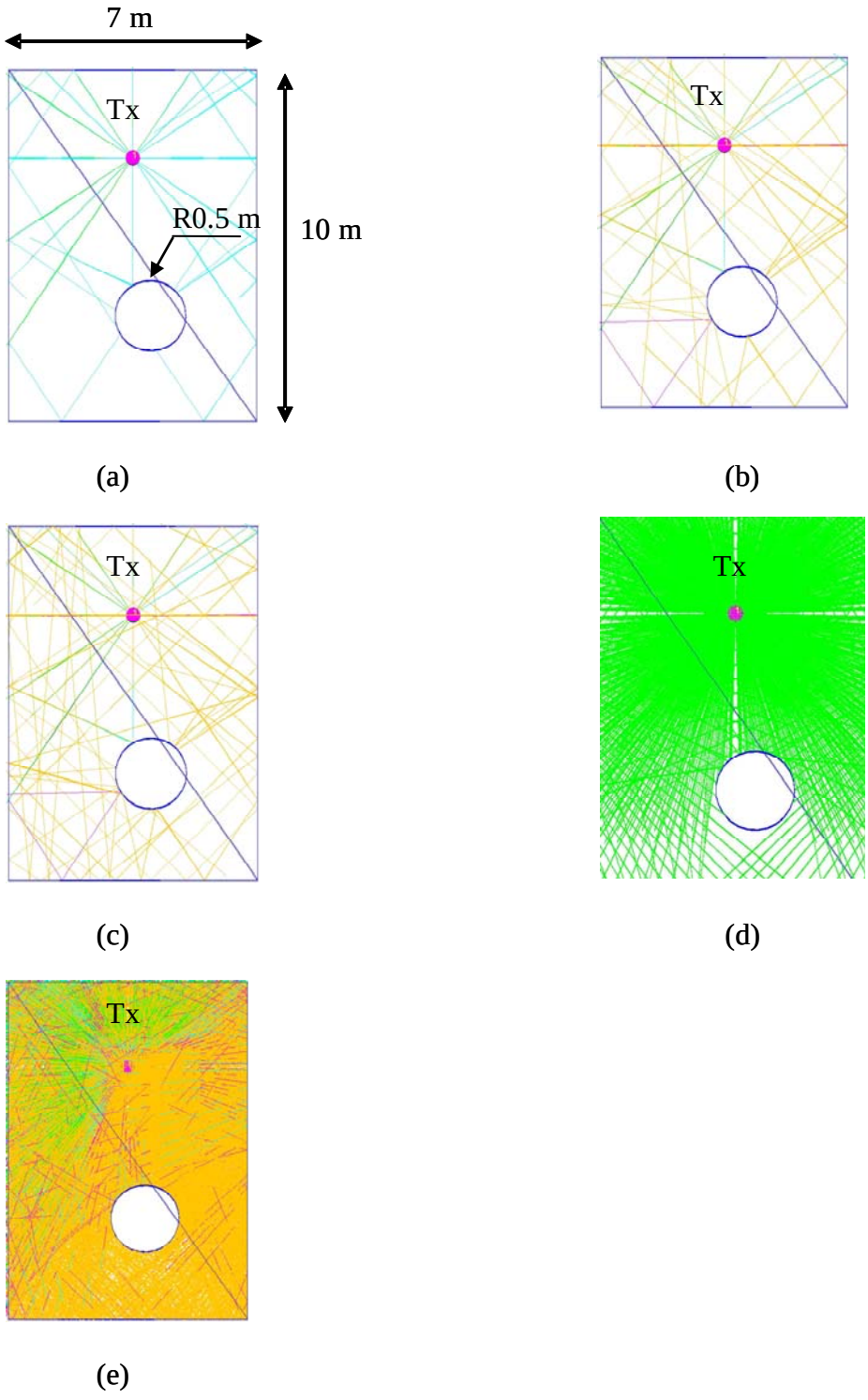

Figure 39. Ray path for (a) two bounces with 30 degree angular interval, (b) four bounces with 30 degree angular interval, (c) 10 bounces with 30 degree angular interval, (d) one bounce with three degree angular interval, (e) five bounces with two degree angular interval.

E. SELECTION OF MATERIAL PROPERTIES

The Urbana code allows the user to input different material properties depending on the ICOAT used for each material. Because this research project investigates the propagation of waves in a ship environment, most materials are assigned ICOT=0 (for a PEC). In a number of simulations, concrete, wood and glass are also used as materials for specific objects. Those objects were assigned coating material codes other than zero or 888 (the default for absorbing facets). For each coating material, the values of the conductivity σ, permittivity ε and resistivity R are input in the Urbana input file. All materials have the same boundary type (iboundary= 3 for slabs with air backing).

F. SELECTION OF FREQUENCY

The last parameter that needs to be selected for the Urbana input file is the frequency. Because the purpose of this thesis is the design of a wireless local area network, three wireless frequency bands were considered: 900 MHZ, 2.4 GHz and 5.8 GHz. This section discusses the pros and cons of each of three frequency bands.

1. The 900-MHz Frequency Band

In the days before the 802.11 standard, a number of wireless networking products that radiate up to 1 W at 900 MHz were competing in the market place. While the data rate can not compare to the modern network systems, the higher power and lower frequency of the 900 MHz systems offer some significant advantages.

As the frequency of a signal increases, the range it can cover at the same power and antenna gains decreases. As a matter of fact, when all other variables are kept equal, a 100-mW signal at 5.8 GHz appears to travel less than fourth the distance of a signal at 900 MHz due to an increase in path loss in Equation (23). In addition, the requirement of having LOS between the transmitting and the receiving antennas is less critical at the lower frequencies than it is at the higher ones. Also, attenuation by materials generally decreases with frequency. The 900-MHz signals can sometimes penetrate obstacles to establish a radio link between two ends that do not benefit from a LOS advantage. More-

over, the 900-MHz systems do not suffer interference from the increasingly crowded 2.4-GHz ISM band.

Nevertheless, these systems suffer a low data rate throughput (less than 2 Mbps) and a very little vendor interoperability. In addition, the 900-MHz hardware has an increasingly limited availability and is more expensive than the typical 802.11b equipment.

2. The 2.4-GHz Frequency Band

Two ubiquitous wireless networking standards use this frequency band, the 802.11b and the 802.11g. The 802.11b standard offers good range and respectable throughput. While it can send frames at up to 11 Mbps, protocol overhead puts the data rate at 5 to 6 Mbps. It operates using direct sequence spread spectrum (DSSS) at 2.4 GHz and automatically selects the best data rate (1, 2, 5.5, or 11 Mbps), depending on the available signal strength. By far, the biggest advantage of the 802.11b standard is its near universal ubiquity in standard consumer devices. Client and access point (AP) gear are astonishingly cheap, and are embedded in many laptop and handheld devices. With hundreds of corporate networks and institutions using it (including the Naval Postgraduate School and many other respected universities), the 802.11b is certainly the most customizable wireless protocol on the planet. It is also the most hackable.

The 802.11g standard is very similar to the 802.11b but much faster. It can achieve data rates of up to 54 Mbps. It uses the Orthogonal Frequency Division Multiplexing (OFDM) encoding of the 802.11a in the 2.4-GHz band, and also falls back to DSSS to maintain backward compatibility with the 802.11b systems. Even though 802.11g systems are still more expensive than the 802.11b systems, prices are expected to fall as more users upgrade their networks to this standard. Because it offers a higher data rate while keeping backward compatibility with the 802.11b standard, the 802.11g standard may become the next massively ubiquitous wireless technology.

3. The 5.8-GHz frequency band

The 802.11a standard uses the same encoding as the 802.11g standard, but operates in a completely different spectrum which is the 5.8-GHz band. While it enjoys freedom from interference with the 2.4-GHz ISM band devices, it suffers from range problems (offers half the range of 2.4-GHz signals for the same ERP), and is not compatible with the 802.11b systems. This standard is significantly faster than the 802.11b standard but achieves comparable data rates (up to 54 Mbps) to the 802.11g standard. It does not enjoy the same backward compatibility though. Because network guests, sailors, and technicians, are most likely to bring with them 802.11b or 802.11g gear, a few dual band APs (or dedicated 802.11g APs) might be necessary to allow guests the use of the network.

4. Conclusion

For the purpose of this thesis, it was decided to use the 2.4-GHz frequency band for the following reasons:

- It presents a much higher data rate throughput than the 900 MHz which allows for the use of data, voice and video applications onboard the ship.
- It offers a perfect range for the application at hand (not too long as the 900-MHz case, nor too short as the 5.8-GHz case).
- Most wireless devices, add-on cards, and APs built today use this frequency band (and most precisely the 802.11b standard).
- The 802.11g standard that uses the 2.4-GHz frequency band promises many of the advantages of 802.11a without significantly increasing the cost or breaking backward compatibility with the ubiquitous 802.11b standard.

G. SUMMARY OF THE INPUT PARAMETERS SELECTION

Based on the analysis conducted in this chapter, a decision on the best input parameters was made. In the remaining simulations conducted in Chapter VII, the following holds true.

- Computation method is UTD (GO enhanced by GTD).
- Frequency is 2.4 GHz.
- Antenna is a vertically polarized half-wave dipole emitting power levels ranging from 0.01 W to 1 W (except for part A.1.c of the simulation chapter where a directional antenna is used).
- All materials have Urbana boundary type 3, denoting slabs with air backing.
- Rays are launched at two-degree intervals and are allowed five maximum bounces.

VII. SIMULATION

The previous chapters described the Urbana code, developed models of shipboard compartments and suggested a set of input parameters to be employed for the simulation part of this thesis. The goal of this chapter is to use those compartments and input parameters to show that propagation simulations are excellent tools to help engineers better assess the performance of a proposed WLAN.

The success of any WLAN is most widely measured by two criteria, good coverage of desired area and security. In the first part of the chapter, Urbana simulation results show the effect of the antenna pattern as well as placement, direct ray contribution, power management, and environment material properties, on the signal distribution throughout different shipboard compartment models. The second part of the chapter treats the problem of insecure, indoor-to-outdoor, outdoor-to-indoor, and indoor-to-indoor propagation of wireless waves, and proposed efficient solutions to increase the security posture of the network.

A. DESIRED COVERAGE AREA

1. Antenna Placement Analysis

The main purpose of this simulation was to investigate the importance of the antenna placement. Optimizing antenna location can reduce multi-path and interference problems. It includes consideration of the antenna height as well as its location relative to nearby objects. In a ship environment, some interference sources are difficult to control and require ensuring a sufficient signal-to noise-ratio (SNR) via the antenna location as well as the gain and the reduction of system loss.

Antenna location optimization requires an evaluation of system coverage and range requirements, a review of station locations, and a review of surrounding objects that may become a source of interference. In the missile room compartment, four simulations were conducted with different antenna locations to emphasize this point. Although they varied in the *x* and *y* positions, all antennas had the same height of 2 m above the ground (the ceiling height is 4 m). The plane of observation points is 1 m above the

ground to simulate the height of a person carrying a hand-held device. The results are shown in the Figures 40 through 43.

The input parameters for this simulation are listed in Table 4.

Antenna locations	Position 1: (7.5 m, 3.5 m, 2.m) Position 2: (9 m, 3.5 m, 2 m) Position 3: (1 m, 6 m, 2 m) Position 4: (3 m, 3.5 m, 2 m)
Antenna type	1 W, $\lambda/2$ dipole
Observation point plane	$x = (-5$ m, 25 m); $y = (-5$ m, 15 m); $z = 1.5$ m
Propagation mechanism	GO with edge diffraction
Material properties	All PEC
Dynamic range	60 dB

Table 4. Input parameters for antenna placement simulation

Although all antenna positions led to satisfactory signal spread throughout the compartment (with signals exceeding 10 dBm in most cases), the influence of the antenna position on the signal level in some areas of the missile room is very evident.

Depending on the required signal level and the coverage area, the calculated signal level from the Urbana results can be used by an engineer to assess the antenna placement options. For the missile room example, Figure 40 shows that the worst overall signal distribution occurs when the antenna is in position 1 (because the antenna is positioned between two missiles). The signal strength at the operating console (as well as most of the right half of the compartment) is relatively weak as compared to the average signal level in the left half of the compartment. The same type of analysis can be made for the antenna in position 2 (shown in Figure 41). When the antenna is placed in position 3 (Figure 42), the opposite scenario occurred (signal is strong on the right side but relatively weak on the left side) merely because the antenna is positioned in the right lower corner of the compartment.

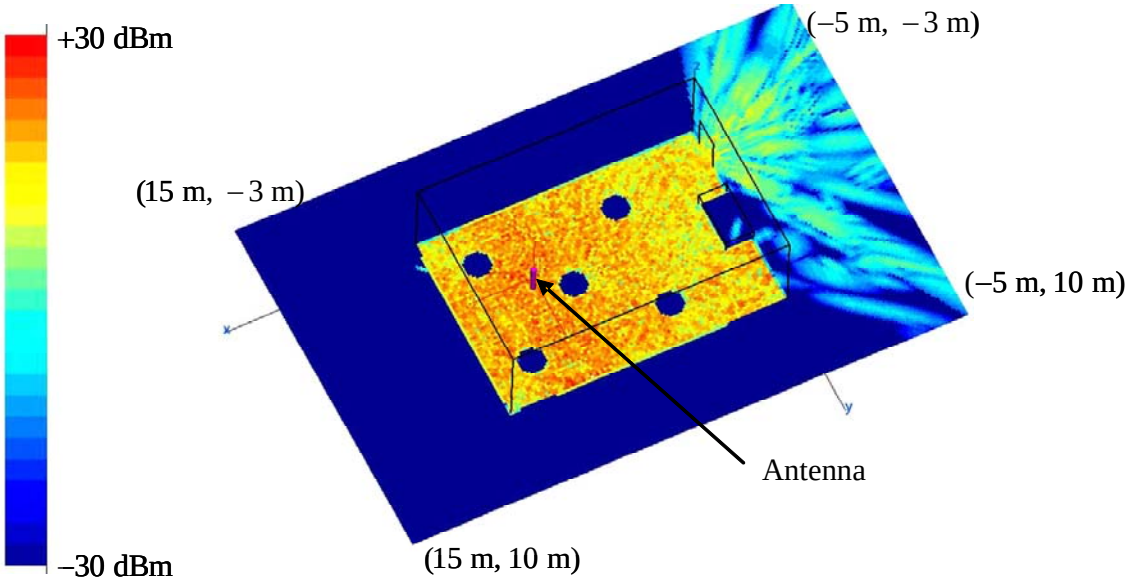

Figure 40. Antenna in position 1

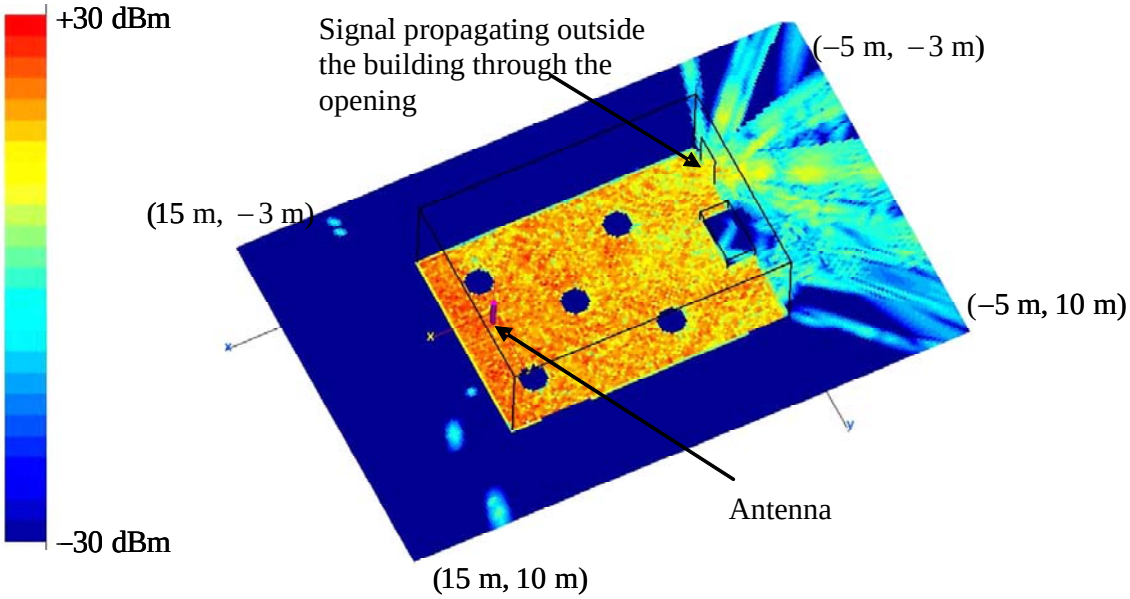

Figure 41. Antenna in position 2

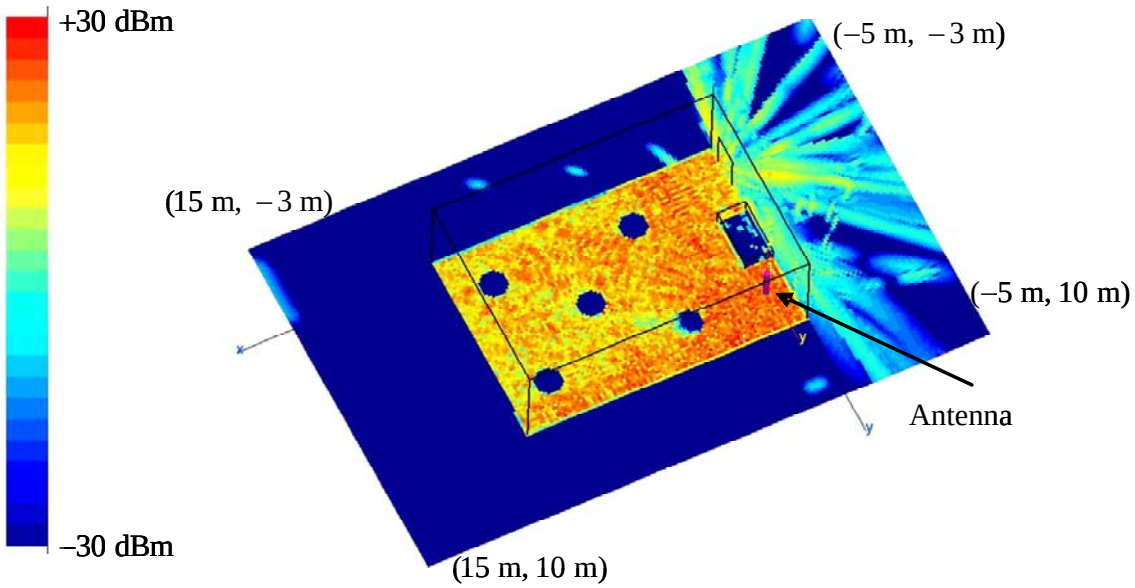

Figure 42. Antenna in position 3

Figure 43 shows that the best area coverage is achieved when the antenna is in position 4. This is due to the fact that the antenna is placed in a slightly open position away from the missiles.

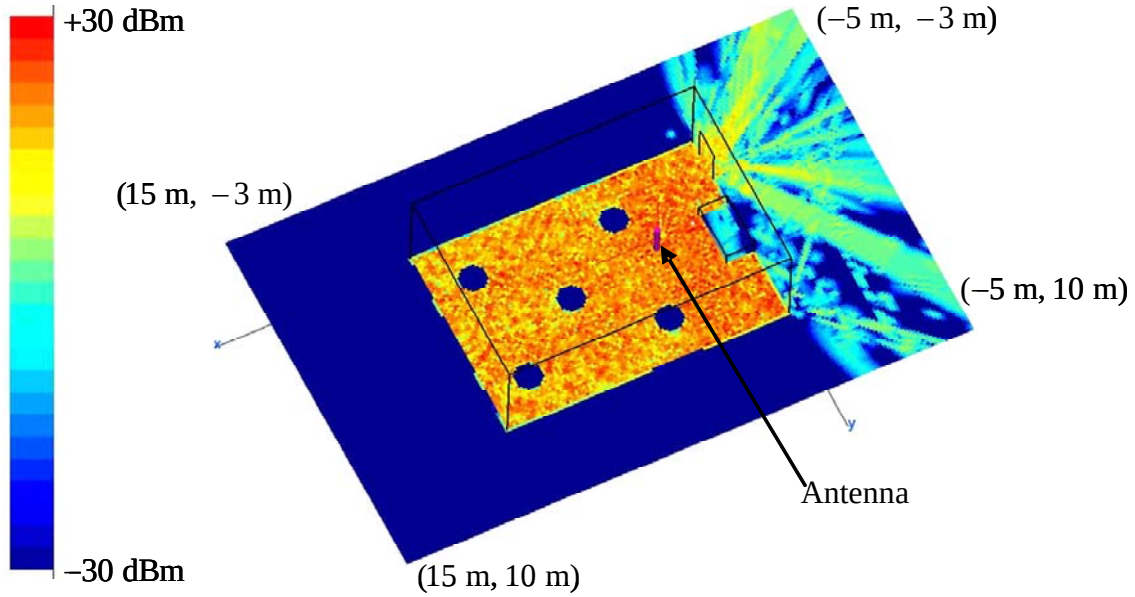

Figure 43. Antenna in position 4

Another nice feature of the Urbana code is its ability to conduct field difference measurements between two simulations covering the same area by using the f2fd program. Figure 44 shows the field difference between the two cases where the antenna is located in positions 1 and 4. By changing the antenna location from position 1 to position 4, the signal level in the left part was improved without too much degradation to the signal level in the right part of the compartment.

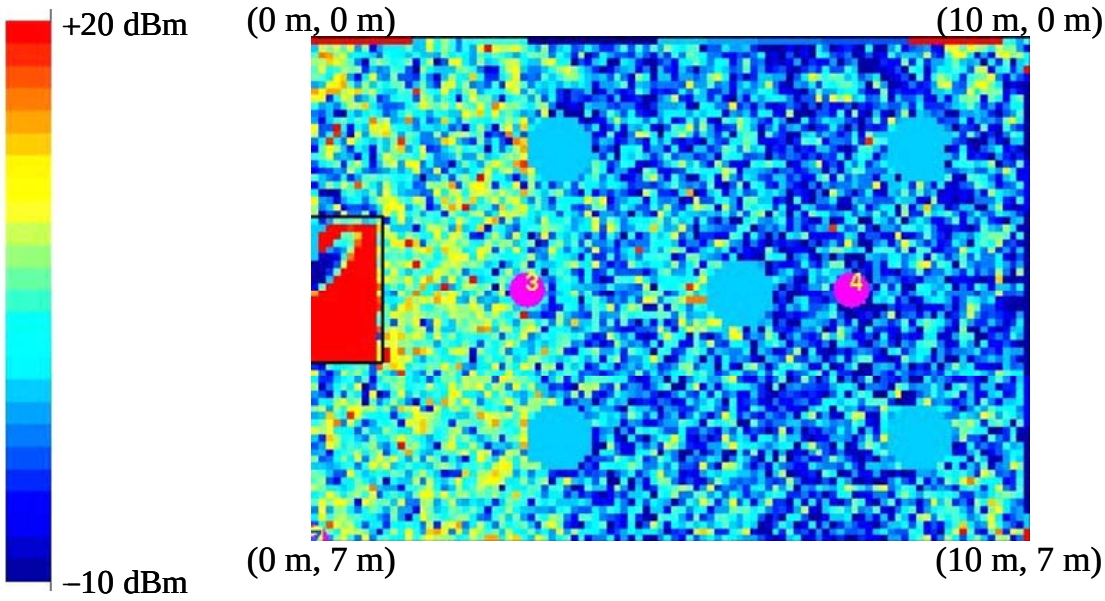

Figure 44. Field difference between antenna positions 3 and 4.

In the design of indoor WLANs that work with mobile communication systems and other portable devices, the most effective placement of the access point (i.e., the antenna in this simulation) is a critical task. It is always desired that computer simulation predicts the coverage of various antenna configurations in order to reduce trial installation and ensure good signal levels in all required areas. The results of the missile room simulations prove that Urbana is an excellent tool that can be used to optimize the antenna location for a particular application. Urbana's analytical results show not only the signal distribution throughout a specific compartment, but the effect of varying this location on the signal level at a predefined set of observation points. This enables the user to conduct comparative analysis and make a decision on the best antenna placement.

The Urbana computational engine is essentially the same as the one for Xpatch, which has been in use since the early 1980s. It has been extensively validated by the elec-

tromagnetic code consortium (EMCC) for radar cross section (RCS) applications. The application of Urbana to indoor propagation problems has been investigated in [20] where it was shown that the predicted fields by Urbana are accurate.

2. Direct Ray Contribution Analysis

The total electric field at each of the observation points is the contribution of direct and scattered (reflected and diffracted) waves that arrive at that point. Although reflected and diffracted waves depend on the geometry of the compartment and the material properties of its different constituents (walls, furniture, etc.), direct rays can easily be predicted.

Figure 45 shows the electric field difference at each of the observation points between the total electric field (with a contribution from incident as well as scattered waves) and the scattered field. The coverage area shows the signal distribution due to direct waves only.

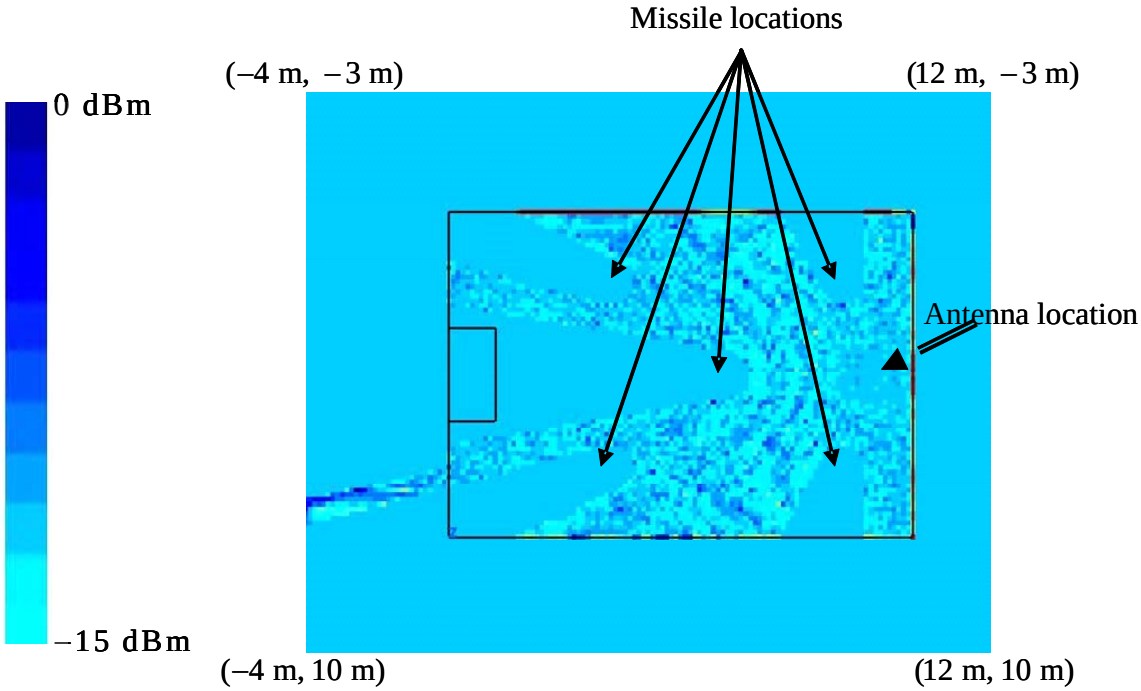

Figure 45. Direct contribution only

It is clear that the areas behind obstacles (pale blue) suffer a strong signal degradation (up to –15 dBm) due to the fact that they do not receive any direct ray contribu-

tion. Areas that have a LOS with the emitting antenna recorded a much higher signal strength. Consequently, it is important to consider this factor when optimizing the antenna location. It is always better (when possible) to expose the direct antenna rays to as much of the space as possible.

3. Directional Antennas

This simulation presents a study of the difference between a directional antenna and a half-wave dipole. The missile room compartment is again used for the purpose of this simulation. The input parameters for this simulation are listed in Table 5.

Antenna locations	(3 m, 3 m.5 m, 2 m);
Antenna type	1 W, Parabolic antenna with 15° HPBW
Observation point plane	$x = (-5 \text{ m}, 25 \text{ m})$; $y = (-5 \text{ m}, 15 \text{ m})$; $z = 1.5 \text{ m}$
Propagation mechanism	GO with edge diffraction
Material properties	All PEC
Dynamic range	47 dB

Table 5. Input parameters for the directional antenna simulation

Figure 46 shows the total electric field distribution in the missile room when a directional antenna is used. It is obvious that most of the energy is focused to the front of the antenna and that the area behind the antenna suffers moderate signal degradation.

Figure 47 shows the results of the same simulation settings as above, but with a half-wave vertically polarized dipole.

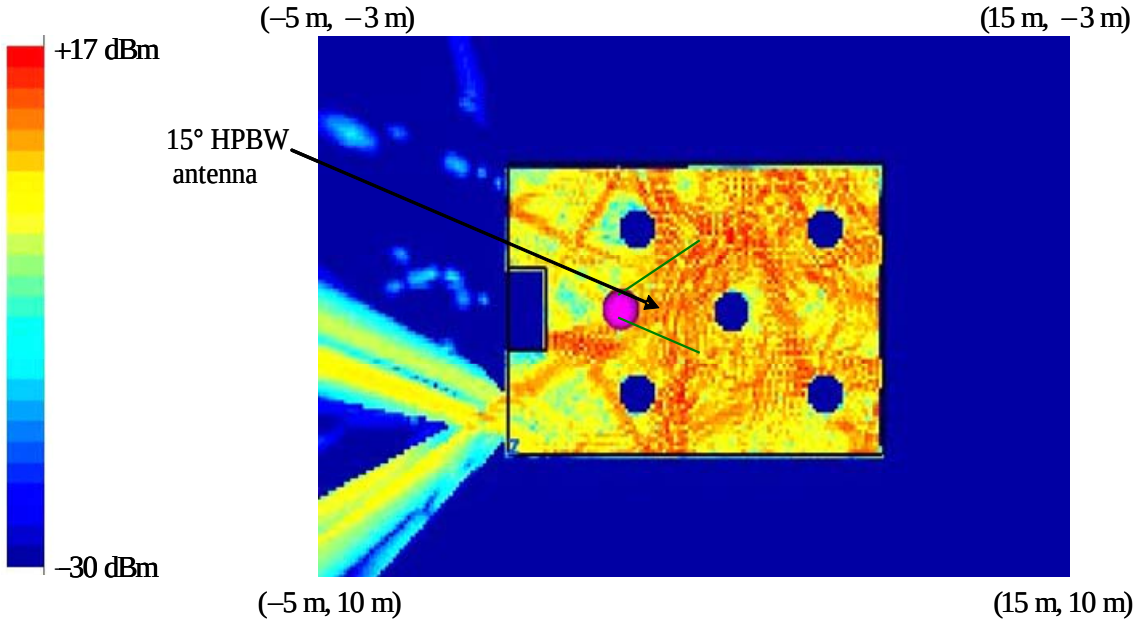

Figure 46. Directional antenna results

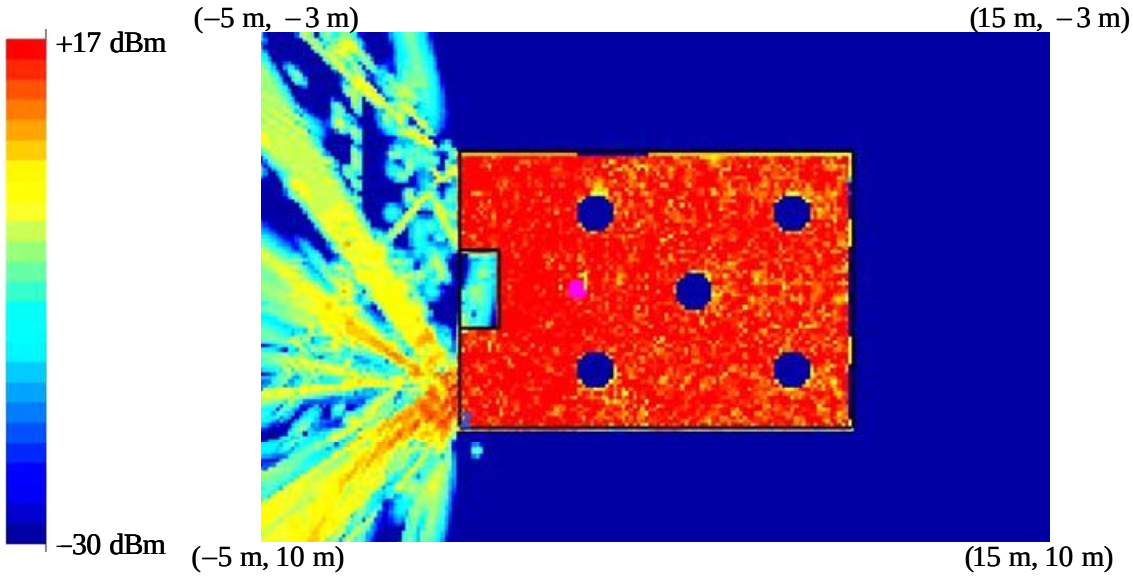

Figure 47. Half-wave dipole antenna results

It is clear that, for this particular case where both antennas are radiating the same ERP, the use of a dipole leads to much better results as far as coverage area goes.

These simulations show that a WLAN designer can use Urbana to analyze the effect of different antenna patterns on the signal distribution in an indoor setting. Based on simulation results, a decision on the best antenna pattern to use can be made.

4. Power Management

In most electromagnetic applications, it is well-known that as the power emitted increases, the signal level at the receiver is improved (when everything else is kept constant). This holds true for a WLAN implementation on board ships. More power usually leads to enhanced area coverage.

In this simulation, the Rhino model of a study area onboard an aircraft carrier was used. The input parameters for this simulation are listed in Table 6.

Antenna location	(10 m, 7.5 m, 1.5 m)
Antenna type	$\lambda/2$ dipole, power varies between 0.01 W to 1 W
Observation point plane	x = (0 m, 20 m); y = (0 m, 15 m); z = 1.5 m
Propagation mechanism	GO with edge diffraction
Material properties	Outer walls: all PEC Inner walls: wood with ε_r = 5 and μ_r = 1
Dynamic range	73 dB

Table 6. Input parameters for power management simulation

Figures 48 through 50 illustrate what happens to the signal distribution inside the compartment as the antenna power is increased from 0.01 W to 0.1 W and finally to 1 W. When 0.01 W of radiated power is used (case of Figure 48), some of the room corners recorded signal levels as low as -50 dBm. Depending on the sensitivity of the receiving wireless device, this signal strength might be lower than the minimum threshold. In this case, the WLAN would have failed to provide good coverage in all areas that were supposed to be covered by the network.

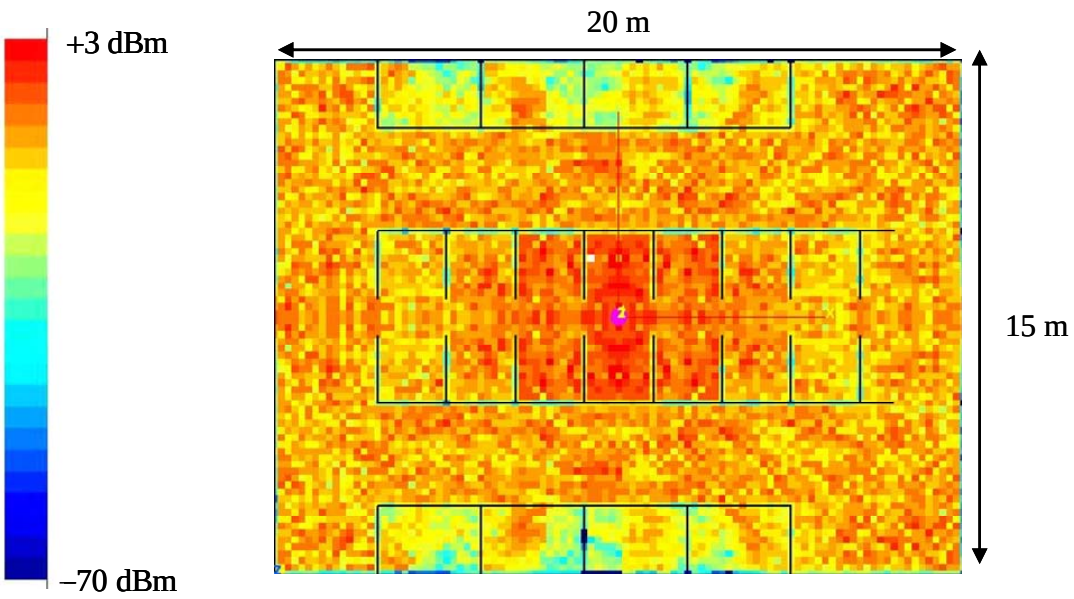

Figure 48. Antenna radiating 0.01 W

Figure 49 presents the results of the simulation when the antenna radiates 0.1 W of power. The same dynamic range is used for this simulation in order to observe the change in field strength. The red areas signify a signal level that is equal to 3 dBm or higher. It is important to remember that 3 dBm is the maximum signal strength recorded with the antenna emitting 0.01 W of power. The antenna radiating 0.1 W of power achieved an average field strength of 10 dBm higher than the antenna radiating 0.01 W. Although the above result is considered good as far as coverage area goes, it has some drawbacks from the security standpoint. More on network security is discussed in the next section of this chapter.

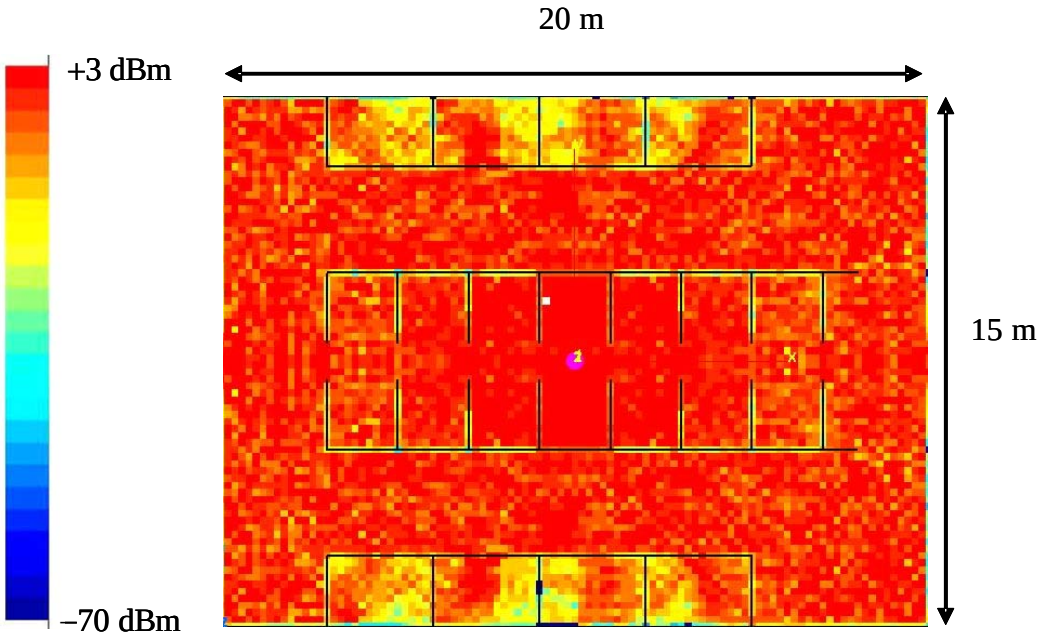

Figure 49. Antenna radiating 0.1 W

Because FCC regulations allow the use of antenna output power up to 1 W without licensing [17], it is sometimes beneficial to make use of this advantage in order to achieve better coverage if security and power consumption are not an issue. Figure 50 shows the signal distribution when a 1-W antenna is used.

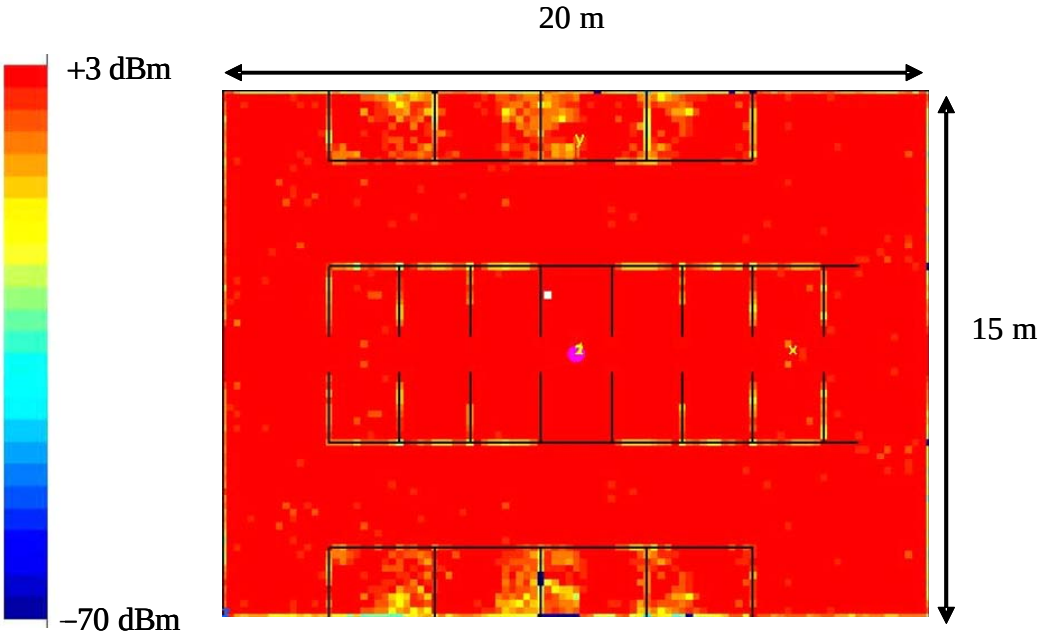

Figure 50. Antenna radiating 1W

The power management simulations show that Urbana can be used to assess the powering requirements of a WLAN antenna in order to achieve a desired signal level and coverage area. An engineer can conduct comparative studies and analyze the performance of a design as the radiated power is varied.

5. Material Selection

Most of the current naval ship compartments are made of steel. In addition, most of the materials that make the inner compartment objects and walls are also made of steel, and can be considered as PEC. This simulation shows that a change in the material properties of some of the inner compartment walls can lead to a big change in the way EM waves propagate and cover a specific area. The input parameters for this simulation are listed in Table 7.

Antenna location	(10 m, 7.5 m, 1.5 m)
Antenna type	$\lambda/2$ dipole radiating 1 W of power
Observation point plane	x = (0 m, 20 m); y = (0 m, 15 m); z = 1.5 m
Propagation mechanism	GO with edge diffraction
Material properties	Outer walls: all PEC Inner walls: PEC (Figure 51) Composite material (Figure 52)
Dynamic range	80 dB

Table 7. Input parameters for material selection simulation

Figure 51 shows the field strength distribution when all materials are considered PEC, while Figure 52 shows corresponding results when all the outer walls are kept PEC and all the inner walls are changed to a composite material with $\varepsilon_r = 5$ and $\mu_r = 1$.

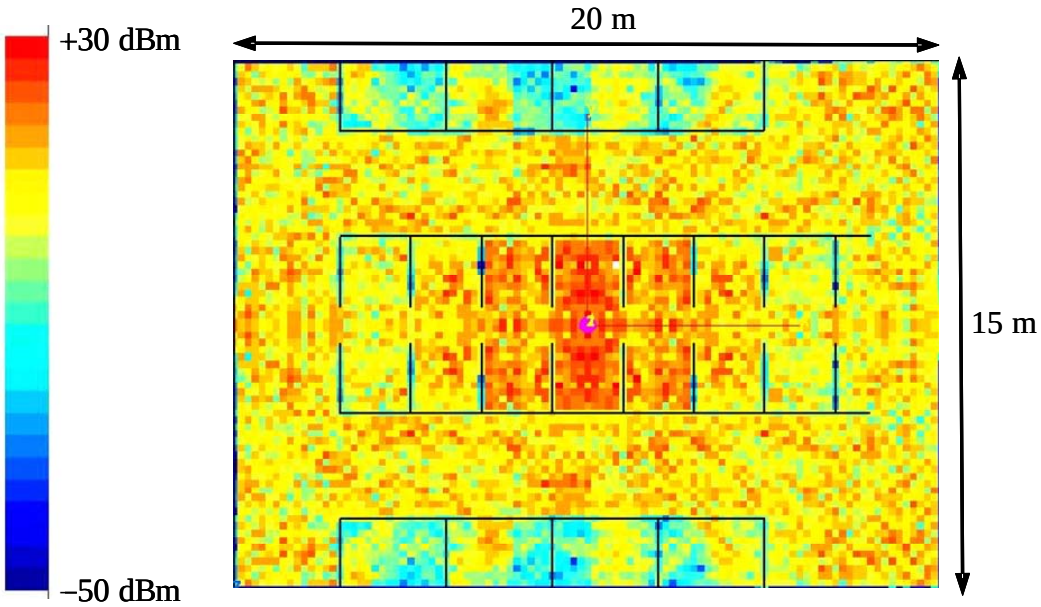

Figure 51. All-PEC field distribution

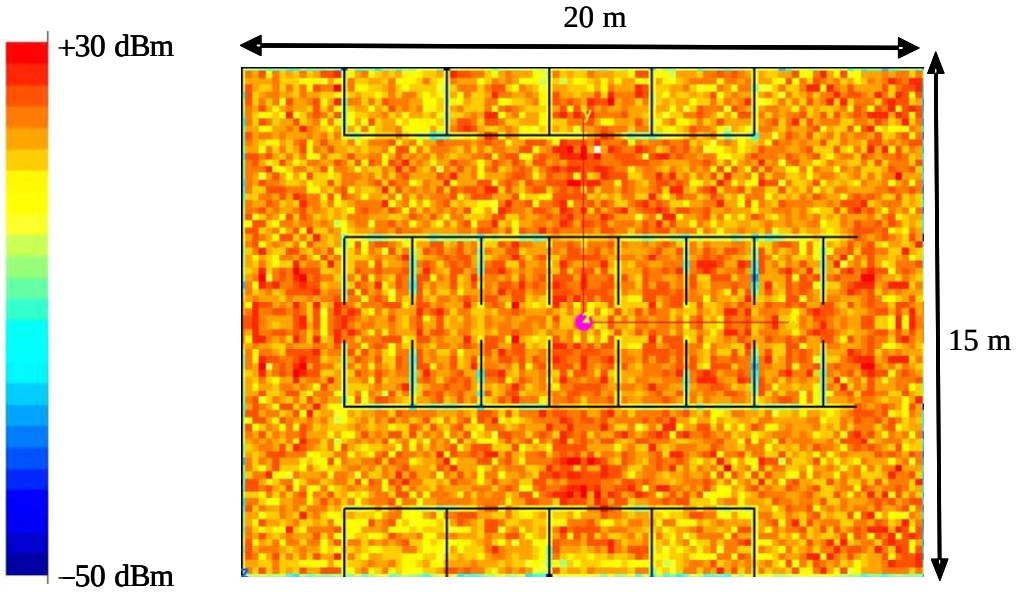

Figure 52. Mix of PEC and composed material field distribution

When using the same dynamic range (– 50 dB to +30 dB) and radiated power (1 W), it is noticeable (from the spread of areas with 30 dBm of signal strength) that this change in material properties has led to a much better area coverage. Figure 53 gives an idea about how much improvement in signal strength is achieved by changing only the material properties of the inner walls. The figure depicts the field difference between the

case when all walls are PEC and when the inner walls are changed to a composite material. Obviously signal levels at the corners of the study rooms (those that suffered the most in the all PEC case) benefited the most form this material change.

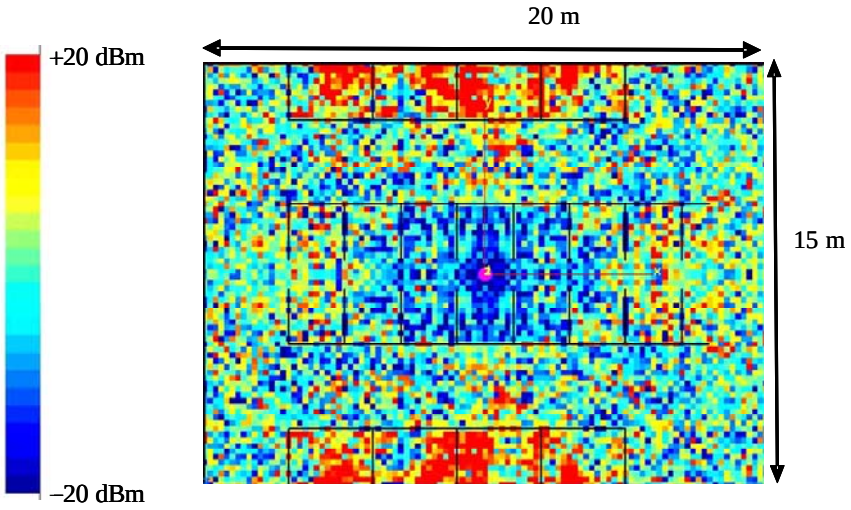

Figure 53. Signal level difference between composite material and all PEC material

Depending on the application and the constraints imposed upon the WLAN designer, this simulation shows how Urbana can be used to predict the area coverage taking into account the material properties of the environment.

B. SECURITY

Once the antenna placement is optimized according to the conclusions derived earlier, it is necessary to look at the wireless propagation of waves from the security aspect. Because signals from WLANs radiate in free space, they can be intercepted by a variety of unwanted intruders from terrorist operatives to sailors that do not have enough privilege to access the network. Those intruders could collect sensitive information and disrupt the ship's network by injecting signals to jam, deceive or take down the network. Although complex encryption techniques make it difficult for the average person to penetrate the network, encryption algorithms built in to the network software are not good enough to withstand an attack by expert hackers.

1. Problem

a. Indoor-to-Outdoor Propagation

In this section, propagation from the inside of the ship to the outside is analyzed using the bridge as an example of a ship compartment equipped with a WLAN. The input parameters for this simulation are listed in Table 8.

Antenna location	(8 m, 6 m, 2 m)
Antenna type	$\lambda/2$ dipole radiating 1 W of power
Observation point plane	x = (–5 m, 15 m); y = (–3 m, 10 m); z = 1.5 m
Propagation mechanism	GO with edge diffraction
Material properties	All PEC
Dynamic range	60 dB

Table 8. Input parameters for the inside-to-outside simulation

Figure 54 clearly shows that strong wireless signals (above the 10 dBm in some areas) manage to escape the locality of the compartment through the two doors. These same signals can be easily intercepted by receivers in the nearby region. The effect of edge diffraction makes this possible over a larger area.

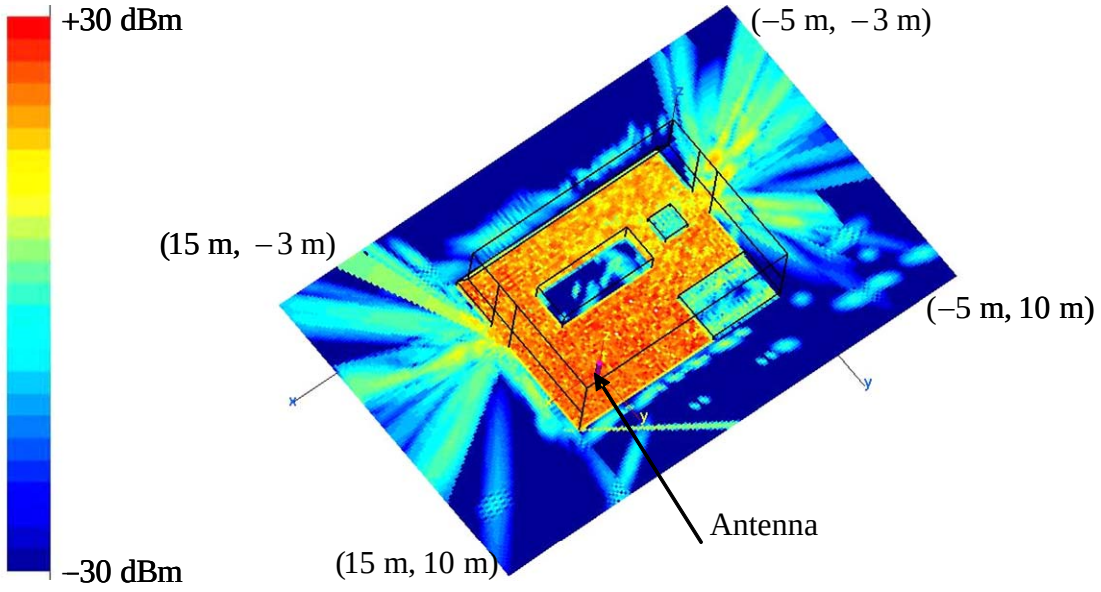

Figure 54. Wireless propagation from inside-to-outside

Any antenna positions other than the one used previously would have led to similar (if not worse) results from the stand point of security concerns. Receivers with crude sensitivities (as low as -50 dBm) would be able to intercept the leaking signals.

b. Outdoor-to-Indoor Propagation

It was shown that waves are easily intercepted if openings are left open. It is important to examine what happens if hidden receivers intercept the signal and inject malicious signals in order to disrupt, deceive or jam the ship's network. Two antenna locations were examined. The input parameters for this simulation are listed in Table 9.

Antenna location	Case 1: (-0.5 m , 2.5 m , 1 m); Case 2: (10.5 m, 2.5 m, 1 m)
Antenna type	$\lambda/2$ dipole radiating 0.1 W of power
Observation point plane	x = (-5 m, 15 m); y = (-3 m, 10 m); z = 1.5 m
Propagation mechanism	GO with no edge diffraction
Material properties	All PEC
Dynamic range	60 dB

Table 9. Input parameters for the outside-to-inside simulation

Figure 55 shows the simulation results when the antenna is placed half a meter outside the compartment in an area easily accessed by unrestricted personnel. Signals enter through the starboard opening, travel through the compartment, go around obstacles, and leave the compartment from the port opening. Note that in this simulation, edge diffraction was disregarded (by not selecting UTD in the input file) to investigate the effects of only the reflected and direct waves. Also, an antenna radiating only 0.1 W was used for this simulation. If edge diffraction was accounted for and a more powerful antenna was used, the results would have been much worst (from the security standpoint).

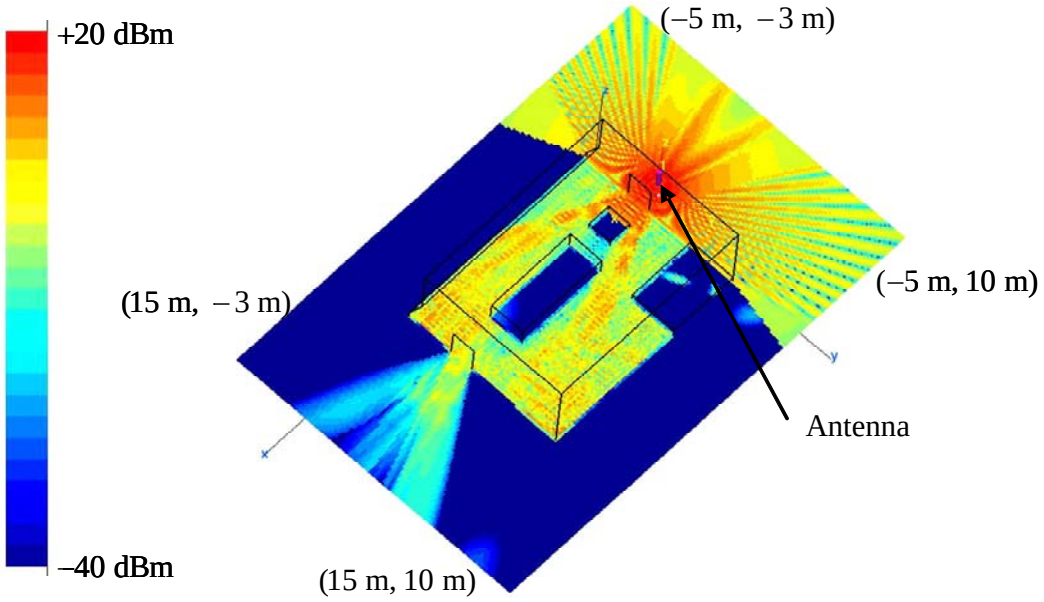

Figure 55. Wireless propagation from outside-to-inside (case 1)

From Figure 55, it becomes apparent that anyone who has access to a half wave dipole emitting a 1 W of power can disrupt the ship's network by injecting signals that can reach all parts of the compartment. The same conclusions can be made when the antenna location moves from the top-right location to the bottom-left as is shown in Figure 56. Signal levels as high +20 dBm could be injected into the ship's network.

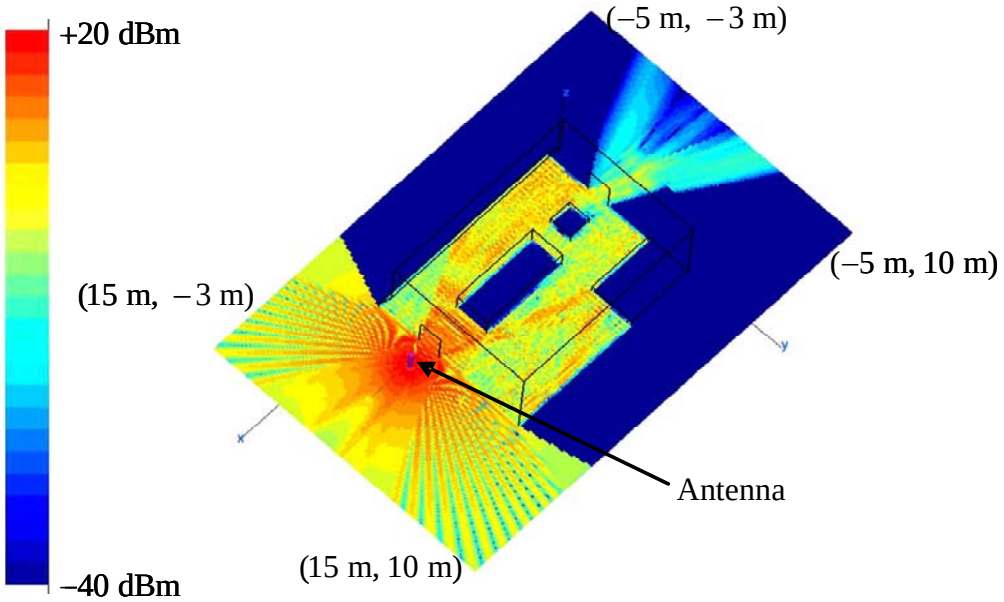

Figure 56. Wireless propagation from outside-to-inside (case 2)

c. Indoor-to-Indoor Propagation

In this simulation, the goal was to investigate how well waves propagate in an indoor environment. The compartment used was the combat information center. This compartment is subdivided into two separate sections, which are accessed by a door as shown in Figure 57. The input parameters for this simulation are listed in Table 10.

Antenna location	(5 m, 6 m, 2 m)
Antenna type	$\lambda/2$ dipole radiating 0.1 W of power
Observation point plane	x = (–1.5 m, 12 m); y = (–3 m, 7 m); z = 1.5 m
Propagation mechanism	GO with edge diffraction
Material properties	All PEC
Dynamic range	60 dB

Table 10. Input parameters for the inside-to-inside simulation

The simulation results show that waves propagate through the opening and make their way around PEC obstacles to cover most of the second compartment. What is even worse is that waves made their way all the way through the second opening to the outside.

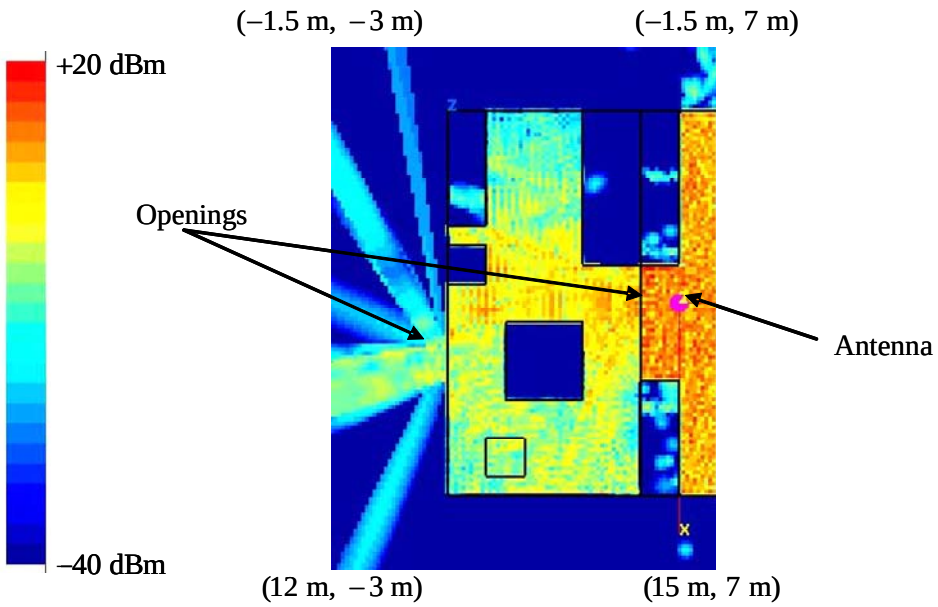

Figure 57. Wireless propagation inside the same compartment

2. Proposed Solutions

a. Placing the Antenna in the Innermost Compartment

Figure 58 shows that as long as there are openings through which waves can propagate, even placing the antenna in the most interior compartment does not prevent signals from leaking to the outside. Signal strength as high as 10 dBm is recorded in some of areas outside the compartment. Depending on the compartment geometry, Urbana lets the user see how well waves propagate from inner compartments through openings.

Based on the coverage results, an engineer can make a decision on whether placing the antenna in the inner most room is a good enough security measure to prevent the network signals from reaching unwanted areas. If that is not good enough, more stringent security measurements have to be implemented.

b. Placing the Antenna Far from the Opening

In this simulation, the CIC_MissileRoom compartment was used. The input parameters for this simulation are listed in Table 11.

Antenna location	(1 m, 6 m, 2 m)
Antenna type	$\lambda/2$ dipole radiating 1 W of power
Observation point plane	x = (–5 m,15 m); y = (–5 m,19 m); z = 1.5 m
Propagation mechanism	GO with edge diffraction
Material properties	All PEC
Dynamic range	60 dB

Table 11. Input parameters for the antenna far from the CIC door simulation

In this case, the antenna is placed as far away from the CIC door as possible. It is in fact placed at the top right corner of the missile room compartment. As shown in Figure 58, almost half of the CIC compartment received good signal strength (above the 0 dBm), while the half that is the farthest from the missile room opening recorded signal strength that is considerably lower than –30 dBm.

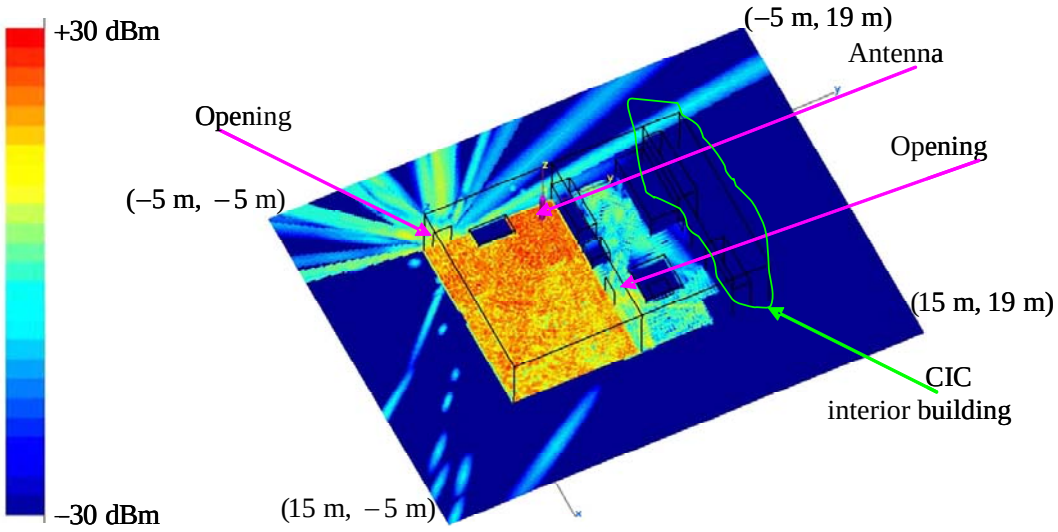

Figure 58. Antenna far away from the opening

Despite the fact that the detected signal inside the CIC is not strong, it is considered good enough to be intercepted by any modern receiver. In addition, by putting the antenna as far from the CIC door as possible, the antenna ended up very close to the outside door, which, in this specific case, made the network more vulnerable by exposing some of its strong signal to the outside world. The conclusion of this simulation is that, although the antenna is placed as far from the CIC opening, sailors residing in the CIC might still pick up the signal generated from the missile room if the CIC door remains open.

c. Closing the Openings

In this simulation, the CIC door was closed. The input parameters for this simulation are listed in Table 12.

Antenna location	(6.5 m, 1 m, 2 m)
Antenna type	$\lambda/2$ dipole radiating 1 W of power
Observation point plane	x = (–5 m, 15 m); y = (–5 m, 19 m); z = 1.5 m
Propagation mechanism	GO with edge diffraction
Material properties	All PEC
Dynamic range	60 dB

Table 12. Input parameters for the case where all doors are closed

Figure 59 illustrates the results of this simulation. No propagation is detected inside the CIC (because all walls and doors are PEC) while waves were able to leak from the missile room to the outside because the outside door is kept open.

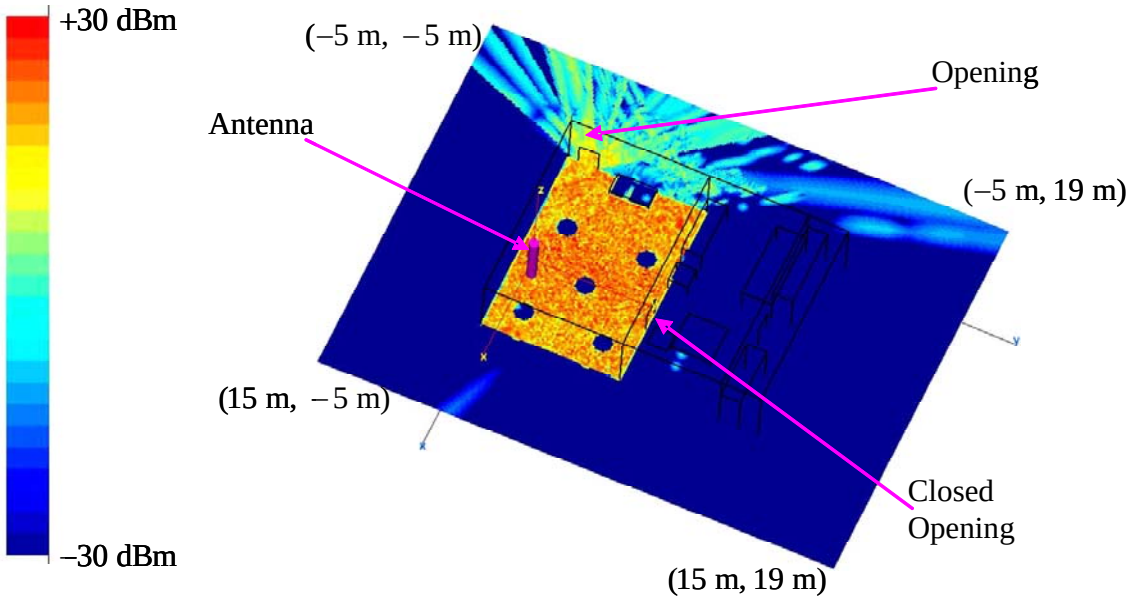

Figure 59. Case where all inner doors are closed

The results of this simulation show that closing the doors or hatches of a compartment is a very effective solution to prevent waves from leaking to the outside of a defined ship environment. Figure 60 shows a secure WLAN environment where no one in the adjacent compartment or on the outside can access the network resources because all doors are closed in this case.

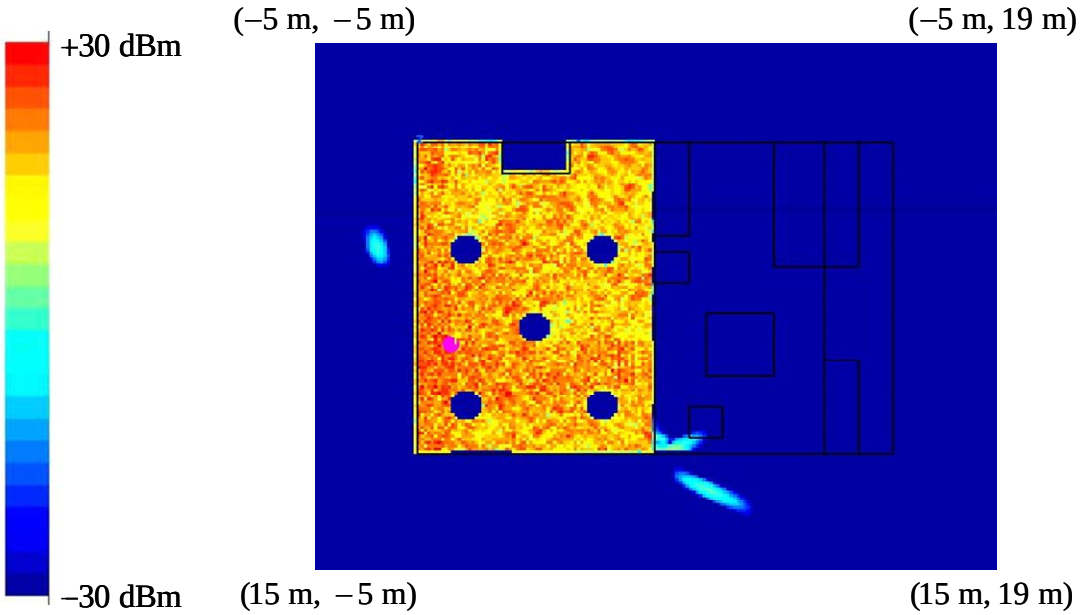

Figure 60. Case where all doors are closed

d. Use of Directional Antennas

Although the use of a directional antenna was not very successful in achieving a good coverage area as discussed in Section A.3 of this chapter, it is known that the use of directive antenna can be very beneficial as far as security is concerned. Figure 46 demonstrated that by limiting the spatial radiation distribution, the average signal level leaving the opening is much weaker than that of Figure 47, where a half-wave dipole was used. As a matter of fact, the main beam of the directional antenna was oriented so that it radiated away from the opening (in exactly the opposite direction) to lower the risk of waves reaching unwanted areas.

Through simulation, an engineer can determine whether a directional antenna is good enough to cover the required area and whether the use of a dipole can lead to a security breach. Then a decision can be made on the best way to proceed with the implementation of the WLAN. Depending on whether security is a concern or a priority, a compromise between security and signal spread has to be reached.

e. Power Management

It was concluded in Section A.4 of this chapter that more power radiated generally means a higher signal at the receiving station. Figure 61 shows the field difference (by using the f2fd application in Urbana) between the cases of using 1-W and 0.1-W antennas. It is clear that a constant 10 dBm average field difference occurs at all observation points by increasing the radiated power 10 times. This is definitely good for users inside the compartment but also leads to higher signal levels on the outside, as seen in the figure.

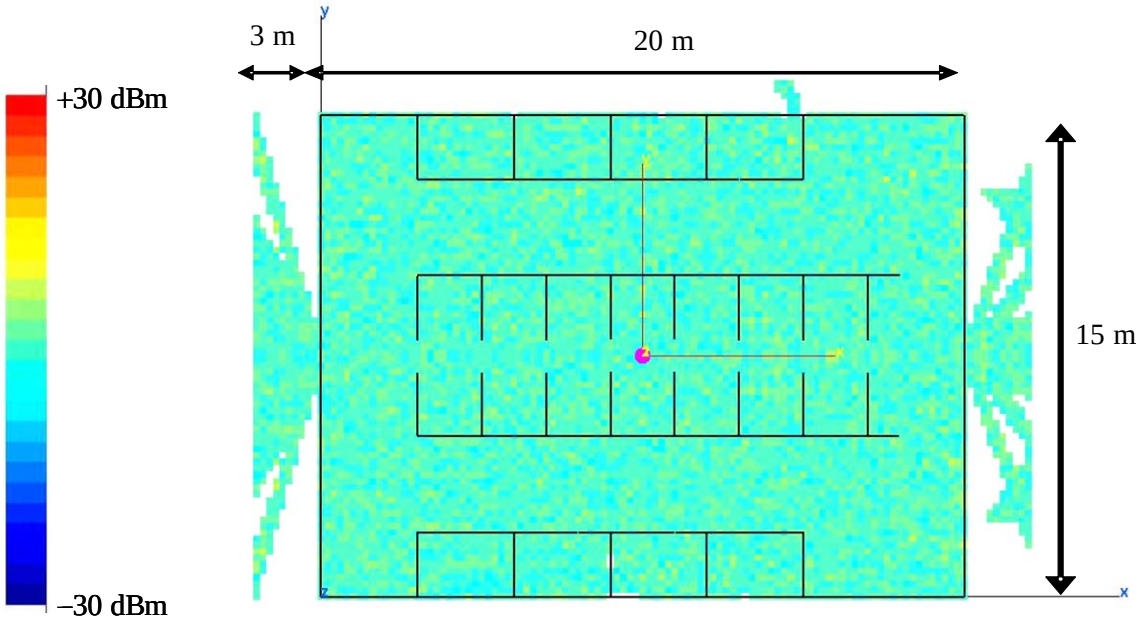

Figure 61. 1-W and 0.1-W antennas field difference results

Sometimes a power increase is compulsory in order to achieve signal level requirements in a specific area. Figure 62 shows how almost six of the eight study rooms have very low signal levels when a 1-W antenna is used. On the other hand, the same antenna provided enough power so that waves with signal levels above 10 dBm leaked to the outside of the compartment through the openings.

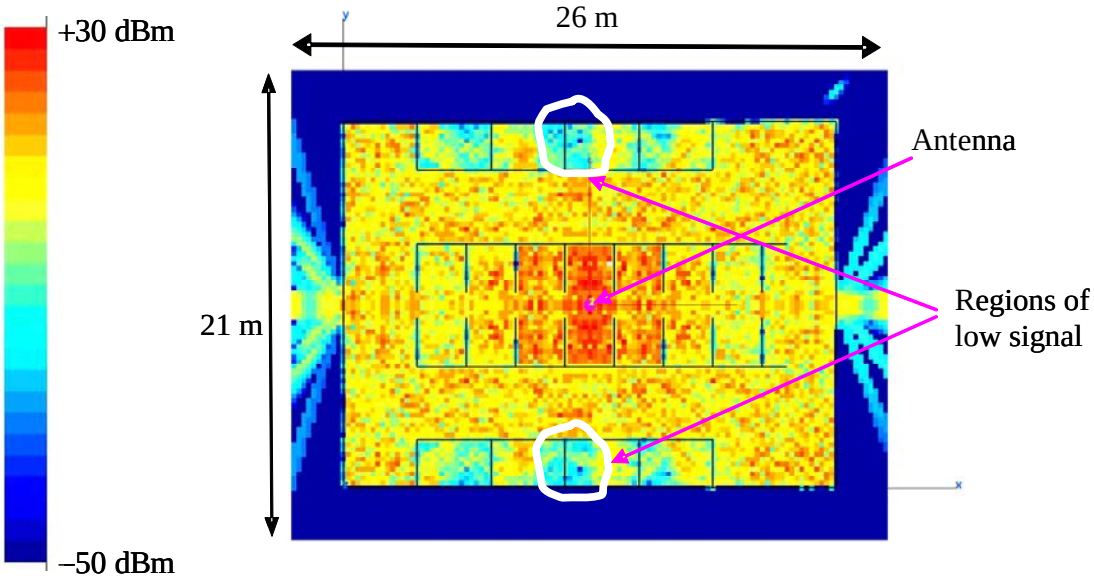

Figure 62. All PEC study space radiated by a 1 W antenna

As this simulation illustrates, confining WLAN signals to a defined area, while at the same time trying to cover the whole space is sometimes not feasible in the presence of openings. A comparative analysis that includes varying one or many of the parameters discussed in this thesis can lead to either solving the problem or at least reducing it to a manageable level.

3. Summary of Security Analysis

According to the results of the different simulations conducted in this chapter, precautions have to be taken to reduce the risk of wave propagation in unwanted areas and to improve the security of a network. These include but are not limited to, locating access points as far from the openings as possible, putting the transmitting antennas in the most interior building, and using sectored access points to limit the spatial radiation distribution. The most effective solution is to completely close all hatches and doors so no EM waves can propagate through the PEC walls to the outside.

The Urbana code has proven very effective in predicting what happens if one or a number of the variable inputs are changed. By providing the user with the signal strength at specific observation points, Urbana helps designers assess the performance of their WLAN in coverage area as well as security requirements.

VIII. SUMMARY AND RECOMMENDATIONS

A. SUMMARY OF RESULTS

The primary objective of this thesis was to investigate the propagation of wireless signals in some shipboard compartments. The Urbana software package was used as the simulation tool. The selection of the IEEE 802.11 standard, and more specifically the 2.4-GHz frequency band, was based on its ubiquitous compatibility with commercially available software and hardware elements, which is an appealing feature for the Department of Defense acquisition process.

In Chapter VI, some simple examples were developed to assess the performance of the Urbana code and validate its use in complex and challenging propagation environments. Then, an analysis of the different possible input parameters to the Urbana input file was conducted. Finally, based on the results of that analysis, a selection of the best input parameters that fit the application of implementing WLANs onboard ships was made.

Because the focus of this research was on a simple site-specific description of a shipboard environment, a variety of models for shipboard compartments were developed in Chapter V. Most models were developed with the Rhino software, but some were built with the Cifer application in Urbana. In Chapter VII, a series of simulations were conducted to assess the signal distribution inside and outside of the compartment models developed earlier, and to evaluate the security posture of the network. Each simulation started with known inputs of the antenna (frequency, location, emitted power and radiation pattern), the specifications of the environment (like the compartment geometry and material properties), and the propagation computation model. The simulation results depicted the signal distribution over a plane of observation points (representing the locations of possible receiving devices), from which the security posture of the WLAN was surmised.

The output results of Urbana showed that this simulation code is a very useful tool for the propagation modeling of wireless waves in shipboard compartments. A network designer can optimize the antenna location, pattern and effective radiated power, and some of the environment characteristics (like the material properties and opening positions), to achieve a required signal distribution level in specific areas. The most useful aspect of the computer simulation is its ability to answer the question: "what happens if one or a number of the input variables are changed?" By providing the user with the signal strength at specific observation points and, most importantly, the signal level distribution over a plane of those observation points, computer simulations help designers assess the performance of a WLAN.

Also, the simulations were useful in predicting the security posture of the network. Based on the spread of the signal level in regions beyond the desired boundaries of an area network (because of openings, material properties of the environment, or power level used), some security measures can be taken to improve the operation of wireless networks on board ships. As was discussed in Chapter VII, these measures include:

- Locating access points as far from the openings as possible.
- Putting the transmitting antenna in the most interior and physically secure part of the ship.
- Using sectored access points to limit the spatial radiation distribution.
- Closing all hatches and doors when propagation outside a single compartment is to be avoided.
- Decreasing the amount of radiated power to the absolute minimum required for coverage.
- Using PEC material for outside walls and for doors and hatches because EM waves do not propagate through PEC material.
- Changing some of the material properties of the environment in order to either achieve a better coverage area inside a compartment or to improve security while maintaining the same radiated power level.

Urbana's ability to answer "what if?" questions every time an input variable changes makes it an outstanding tool that can be used for the modeling of wireless propagation in shipboard compartments.

The major drawback of the Naval Postgraduate School Urbana code is that most of the simulations were time consuming. This was primarily due to using an older version of the software on SGI Octanes (300 MHz CPUs). Depending on the complexity of the model, the number of the observation points, the computation method, and the computer used, most simulations had run times ranging from one hour to six hours.

B. FUTURE WORK

One important practical problem that causes trouble when implementing a WLAN is Electromagnetic Interference (EMI). This problem was not treated in this thesis. EMI is the disruption of operation of an electronic device when it is in the vicinity of an electromagnetic field in the radio frequency spectrum that is caused by another electronic device. The internal circuits of diverse electronic devices generate EM fields in the RF range. Also, cathode ray tube displays generate EM energy over a wide band of frequencies. These emissions can interfere with the performance of sensitive wireless receivers nearby.

Likewise, high-powered wireless transmitters of radar and communication systems can produce EM fields strong enough to disrupt the operation of other electronic equipment nearby. This could be a fundamental problem when dealing with wireless devices that might be influenced by operational equipment crucial to the mission of the ship (like radars and other combat systems).

Ensuring that all electronic equipment is operated with a good electrical ground system can minimize problems with EMI. In addition, cords and cables connecting the peripherals in an electronic or computer system should be shielded to keep unwanted RF energy from radiating.

Future work that follows what is done in this thesis might focus on the effect of interference in implementing a WLAN. The Urbana code can be used to predict fading and co-channel interference and to conduct parametric analysis to lessen the effect of such a problem on the performance of a desired WLAN.

THIS PAGE INTENTIONALLY LEFT BLANK

APPENDIX

This Appendix includes an example of the Urbana input file and two Matlab codes, one to create the plane of observation points, and the other to generate the pattern of a user defined directional antenna.

A. SAMPLE URBANA INPUT FILE

```
--- input Urbana v 2.5
#
# ********************************
# A---scatterer file,length & freq
# ********************************
#--- name of scatterer file in ACAD format (e.g. wall.facet)
bldg.facet
#--- length unit:1=inch, 2=cm, 3=meter, 4=mm, 5=mil
3
#--- uniform freq (GHz): start freq, end , nstep
#    (nstep=0 means: just do first freq. CAUTION: antenna patterns are
#     assumed to be indep. of freq and is calculated at end freq)
2.4 2.4 0
#
# ********************************
# B--- Antenna Description and List
# ********************************
#
#---Enter method of describing antennas.
#   (1 = here, 2 = file):
1
#---If described in file, enter file name:
dummy.antenna
#---If described here, fill in sections B1, B2, B3.
#   If described in file, use dummy data in sections B1, B2, B3
#   (specify one dummy antenna type, dummy antenna origin,
#    and one dummy item in antenna list).
#
# ************************
# B1: Define Antenna Types
# ************************
#
#   Two lines for each type.
#     Line1: type ID, ant code
#     Line2: parameters
#
#   Type ID must start from 1 and increment by 1 thereafter
#
#   Ant Code   meaning            parameters
#   --------   ----------------   -----------------------------
#      1       pattern file       filename(ascii)
#      2       dipole             length(real)
#
```

```
#   Antenna Types list:
#
#   Enter number of antenna types:
1
#   Type #1
1 2
0.0625
#
# ***********************************************
# B2: Enter origin of antenna coord in main coord
# ***********************************************
#
0.0 0.0. .0
#
# ***********************
# B3: Create Antenna List
# ***********************
#
#   Three lines for each antenna.
#     Line1: Type ID, location (x,y,z), power (watts), phase(deg)
#     Line2: Local x-axis in main coord.
#     Line3: Local z-axis in main coord.
#
#   Enter number of antennas:
1
#
#   Antenna #1
1  50.0 50.0 30.0  1. 0.
1. 0. 0.
0. 0. 1.
#
# **********************
# C---Observation points
# **********************
#--- Observation points defined with respect to main coord. system 7.
#    Enter method of specifying list of points.
#    (1 = here, 2 = file):
2
#--- If points are listed here, enter number of points (kobtot):
1
#--- If listed here (1 above), List xyz of points in main coord 7
#    (one point at a line). If 2 above, include one dummy line.
1.            2.               -11.00
#--- If points listed in file (2 above), enter name of file.
bldgobv.list
#--- Include direct Tx to observer contribution.
#    If you turn on the direct contribution from the transmitter to the
#     observation point, computed result will be the total field, which
is
#     the incident + scattered field.    For propagation analysis, this
is
#    the preferred setting.  Otherwise, the result only includes the
#    scattered field.
#
#     Include direct contribution from transmitter to observation point
(rx)
#    (1 = yes, 0,2 = no):
```

```
1
#--- Compute received power into Rx antenna.
#    Urbana always computes field levels at the observation point.
#     If you specify an Rx antenna, Urbana will also compute the re-
ceived
#    power and record the results in the (runname).couple file.
#     This causes a moderate but slow-down when using the SBR method
(below).
#
#    Include Rx antenna (1 = yes, 0,2 = no):
0
#--- Rx antenna specification
#    Remaining entries in Section C can be ignored if not including
#    an Rx antenna.
#    Enter antenna type (1 = pattern file, 2 = dipole):
2
#    Each antenna type requires additional parameters.
#    List of expected parameters follows.  Choose one.
#
#    Type  Description     Expected Parameter(s)
#    1     Pattern File    File Name (e.g., beam.antpat)
#    2     Dipole          Length (in prevailing unit)
#
#    Enter parameter(s) on next line:
2.5
#--- Rx antenna orientation
#    Enter local x-axis of Rx in global coordinates
1. 0. 0.
#    Enter local z-axis of Rx in global coordinates
0. 0. 1.
#
# ****************************
# D---Theoretical consideration
# ****************************
#--- Choose method of computation
#    0 = compute fields in the ABSENCE of the scatterer
#    1 = compute fields by SBR
#    2 = compute fields by GO
2
#--- If SBR, select a PO integration scheme at bounce points
#    1 = do integration at first & last bounce points only
#    2 = do so at all bounce points (GTD formulation)
#    3 = do so at all bounce points (PTD formulation)
2
#--- Edge diffraction
#    SBR can be enhanced with PTD edge diffraction.
#    GO can be enhanced with GTD edge diffraction.
#    Add edge diffraction (0,2=no, 1=ILDC (SBR or GO), 3=UTD (GO only)
3
#--- If edge diffraction switched on, enter name of edge file
#    (e.g., wall.edge or dummy if edge not included).
bldg.edge
#--- Choose method of ray launch
#    1 = by (baby) facet, achieving a uniform first bounce surface den-
sity
#    2 = uniform angular distribution (burst launch)
#    (If computation by GO, must select 2 = burst launch)
```

```
2
#--- If ray launch by (baby) facet (1 above), enter ray density:
#    # rays/wavelength (normally 5-10)
5.
#--- If burst ray launch (2 above), enter angular interval (deg).
#    (Typically 0.25 - 2.0 deg)
2.
#--- max permissible ray bounces (normally 5-10)
5
#--- max-voxdepth = max depth of BSP tree (normally 20)
#    max-voxl = max facets in each voxel(normally 10)
#    (Larger voxdepth & smaller voxl lead to faster ray tracing
#     but more computer memory)
20,10
#--- ICOAT for absorbing facets
888
#--- IQMATRIX for divergence factor
#     1 = calculated by Q-matrix
#     2 = ignored except for the spherical wave spread
2
#--- IF using Q-matrix, name target curvature file(e.g. wall.curv)
dummy.curv
#--- IPEC=1 if all pec,  =2 if coating present
1
#--- For PEC scatterer, give the magnitude of reflection coeff
#    (use 1.0 for ideal PEC, use less for rough PEC--fudging)
1.
#--- IF PEC, the rest coating info is dummmy
#--- material reflection is done through a look-up table
#    specify the freq interval in GHz for the table e.g. 0.25
#    (dummy if input freq less than 51)
0.2
********************
E---coating material
********************
---- number of materials
      (NOT including pec, which is identified by ICOAT=0)
      (NOT including absorbing facets:  ICOAT=28 or 888)
      (If 3 material, urbana reads only ICOAT=1-3)
1        <----NCOTOT
--- for each material, identify its boundary type:
    iboundary = 1 if impedance boundary
                2 if layered slabs with PEC backing
                3 if penetrable layered slabs with air backing
                4 if penetrable FSS Tx/Refl table supplied by user
                5 if same as 2 except using freq-dep ramlib.d
                6 if antenna refl table supplied by user
                7 if layers over semi-infinite ground
# for each material, given info by following the templates
^^^ ICOAT=1 ^^^^^^^^^^^^^^^^^^^^^^^^^^^^^^^^^^^^^^^^^^^^^^^^^^^^^^^^
--- iboundary
3
--- number of layers over air backing
    (1st layer is farthst fr incid field and innermost)
1
--- thick,epsilon(c),mu(c),resistivity(ohm)
6.00 (5.5,-.5) (1.0,0.0) 1e30
```

```
(End of regular input file. Leave a few blank lines)



-----------------------------------------------------------------
'OPTIONAL ADVANCE FEATURES' (Do not change letters in quotations)
# The line above must be placed at the end of the regular urbana
# input. Advance features are designed for special applications or
# for testing codes.  They are not needed by general usages.
# ------------------------------------
# ADVANCE1: ADD GTD-TYPE BLOCKAGE CHECK
# ------------------------------------
# In regular urbana computation, blockage check is mostly done by
# PTD principle. For interior scattering in a confined region, use of
# GTD principle may be more appropriate.
# Option to use GTD principle:  1=yes,    2=no (regular case)
2
# ---------------------------------------
# ADVANCE2: SIMPLE TERRAIN BLOCKAGE MODEL
# ---------------------------------------
#  For  GO  method,  terrain  generates  100%  blockage,  and  blocked  rays
leave
# no energy behind a hill.  With this feature, LOS rays and UTD edge
# diffraction rays can pass through terrain, with some attenuation.
# Attenuation is measured in dB per hill.  Each hill is identified
# by two passages through two terrain facets.
# Can only be used with GO method (and UTD edge option).
# Use simple terrain model: 1 = yes, 2 = no (regular case)
2
# Enter coating code range of terrain facets (e.g., 1, 2):
1 1
# Enter amount of attenuation per hill (dB, > 0):
5.
# ------------------------------------------------
# ADVANCE3: APPROXIMATE DOUBLE DIFFRACTION MODEL
# ------------------------------------------------
# For GO + UTD method, only single diffraction is considered.
# With this feature, double diffraction is approximated by identifying
# surfaces which block the single diffraction, such as building walls.
# If one or two facets block the path from the single diffraction point
#  to  the  transmitter,  the  diffraction  is  still  included,  but  with  at-
tenuation.
# Works best if "diffracting facets", marked by their coating code, are
# always associated with enclosed structures with well defined edges.
# Use double diffraction model: 1 = yes, 2 = no (regular case)
2
# Encounter coating code range of diffracting facets (e.g., 5, 10):
2 2
# Enter amount of attenuation for second diffraction (dB, > 0);
10.
# ----------------------
# ADVANCE4: ACCELERATION
# ----------------------
# For large scenes, run time grows both with the number of field
```

```
# observation points and the number of edges.  Normally, all combina-
tions
# of lit edges and observation points are considered.  This feature
# accelerates the processing by limiting the scope of considered edge
# interactions to region around the LOS path from the transmitter
# to the observation point.  For example, to run a 5 km by 5 km scene,
# one may choose a 250 m interaction radius.  For each observation
# point, edges are ignored that lie outside an ellipse whose foci are
the
# Tx and the observation point and whose major axis is the LOS distance
# plus 500 m (radius x 2).
# This feature can also be used to automatically filter edge files
# whose domain far exceeds the domain of ovservation points.
# Only use this feature for terrestrial simulations where the scene
# is nominally parallel to the x-y plane.
#
# Use large scene acceleration: 1 = yes, 2 = no (regular case)
2
# Enter radius of interaction
250.
```

B. OBSERVATION POINTS GENERATION FILE

```
% Observation points generation
%-------------------------------------------------------------------
---------
clc;
clear;
i = 1;
z = 1;
for x = -2:.2:22;
    for y = -2:.2:17;
        M(i,:) = [x, y, z];
        i = i + 1;
    end
end
save obvpointme M -ASCII;
      %-----------------------------------------------------------------
```

C. ANTENNA PATTERN FILE

```
% Generate Antenna Pattern File for Urbana
clc;
clear;
warning off;

lamda = (3*10^8)/(2.4*10^9);
HPBW = 15; % in degrees
a = 58.4 * lamda / (2*HPBW); % Uniform Circular Aperature Size (radius)
beta = 2*pi/lamda;
E0 = 1;
c = j*beta*E0*pi*a^2/(2*pi); %Contant term in E field
```

```
Directivity = (4*pi*pi*a^2)/lamda^2
Directivity_dB = 10*log10(Directivity)

step1 = 90; %Vertical Steps
step2 = 180; %Horizontal Steps
d_theta = 180/(step1);
d_phi = 360/(step2);
k = 0;
ip = 0;
iq = 0;

    for phi = 0:d_phi:360
      for theta = 0.01:d_theta:180.01 %plots out the zero point
           k = k+1;
f=2*besselj(1,beta*a*sin(theta*pi/180))/(beta*a*sin(theta*pi/180));
           e_theta = cos(phi*pi/180)*c*f;
           e_phi = -sin(phi*pi/180)*cos(theta*pi/180)*c*f;
           if theta > 90
               e_theta = 0;
               e_phi = 0;
           end
           if phi == 0
               ip = ip + 1;
               et0(ip) = 20*log10(abs(e_theta));
               ep0(ip) = 20*log10(abs(e_phi));
               eth(ip) = theta;
           end
           if phi == 90
               iq = iq + 1;
               et90(iq) = 20*log10(abs(e_theta));
               ep90(iq) = 20*log10(abs(e_phi));
               eth90(iq) = theta;
           end
              A(k,1:4)  =  [real(e_theta),  imag(e_theta),  real(e_phi),
imag(e_phi)];
       end
   end

   save antennapat2 A -ASCII;

   figure(1)
   plot(eth,et0,eth,ep0)
   legend('etheta','ephi')
   xlabel('Angle in Degress')
   ylabel('Relative Pattern, dB')
   axis([0,180,-60,20])
   title('phi=0')
   figure(2)
   plot(eth90,et90,eth90,ep90)
   legend('etheta','ephi')
   xlabel('Angle in Degress')
   ylabel('Relative Pattern, dB')
   axis([0,180,-60,20])
   title('phi=90')
```

THIS PAGE INTENTIONALLY LEFT BLANK

LIST OF REFERENCES

[1] A. Goldsmith, “Wireless Communications,” Technical Report, Stanford University, 2004.

[2] Helicomm, “Standard Based Wireless Networking,” presented at the Remote 2004 Conference on Onsite Power for Mission-Critical Equipment and Facilities, San Antonio, November 2004.

[3] P. P. Sumagassy, “Vulnerability of WLANs to Inteception,” Master’s thesis, Naval Postgraduate School, Monterey, California, September 2002.

[4] D. C. Jenn, *Radar and Laser Cross Section Engineering*, American Institute of Aeronautics, Washington, 1995.

[5] D. C. Jenn, Notes for EC3630 (Radio wave Propagation), Naval Postgraduate School, 2004 (unpublished).

[6] B. Harney, Notes for TS3000 (Combat Systems), Naval Postgraduate School, 2004 (unpublished).

[7] K. Siwiak, *Radiowave Propagation And Antennas for Personal Communications*, 2nd edition, Artech House, Boston, 1998.

[8] W. L. Stutzman and G.A. Thiele, *Antenna Theory and Design*, 2nd edition, Wiley & Sons, Inc., Hoboken, NJ, 1998.

[9] J. Martinos, “Prediction of Wireless Communication Systems Performance in Shipboard Compartments in the 2.4-GHz ISM Band,” Master’s thesis, Naval Postgraduate School, Monterey, California, 2001.

[10] M. Hata, “Empirical formula for propagation loss in land mobile radio services,” *IEEE Trans. on Vehicular Technology*, Vol. VT-29, No. 3, pp. 317-325, Aug. 1980.

[11] W. Honcharenko and H. Bertoni, “Mechanisms governing UHF propagation on single floors in modern office buildings,” *IEEE Trans. on Vehicular Technology*, Vol. VT-41, No. 4, pp. 496-504, Nov. 1992.

[12] W. Honcharenko, “Modeling UHF radio propagation in buildings,” Ph.D. Dissertation, Polytechnic University, 1993.

[13] D. Molkdar, “Review on Radio Propagation into and within Buildings,” *IEE Proceedings-H*, Vol. 138, No. 1, pp. 65-68, Feb. 1991.

[14] “Urbana Wireless Tool Toolset Training Handout,” Science Application International Corporation (SAIC), San Diego, October 2004.

[15] Urbana 3-D Wireless Toolkit, http://www.saic.com/products/software/urbana/, last accessed March 2005.

[16] Rhinoceros 2.0, http://www.rhino3d.com/whatnew2.htm, last accessed March 2005.

[17] FCC Rules and regulations, http://www.fcc.gov/searchtools.html#rules, last accessed February 2005.

[18] W. Lee and Y.Yeh, “Polarization diversity system for mobile radio,” *IEEE Trans. on Communications*, Vol. COM-20, No. 5, pp. 912-923, Oct. 1972.

[19] D. Chizhik, J. Ling, and R. Valenzuela, “The Effect of Electric Filed Polarization on Indoor Propagation,” Lucent Technologies, Bell Laboratories, http://www.bell-labs.com/org/wireless/wisepub/icupc98.pdf, last accessed February 2005.

[20] R. Kipp and M. Miller "Shooting and Bouncing Ray Method for 3D Indoor Wireless Propagation in WLAN Applications," *2004 IEEE AP-S International Symposium Digest*, Monterey, CA, June 2004.

INITIAL DISTRIBUTION LIST

1. Defense Technical Information Center
   Ft. Belvoir, VA

2. Dudley Knox Library
   Naval Postgraduate School
   Monterey, CA

3. Chairman, Electrical and Computer Engineering Department
   Code EC
   Naval Postgraduate School
   Monterey, CA

4. Chairman, Information Sciences Department
   Code IW
   Naval Postgraduate School
   Monterey, CA

5. Professor David C. Jenn
   Code EC/Jn
   Naval Postgraduate School
   Monterey, CA

6. Professor Curt D. Schleher
   Code IS/Sc
   Naval Postgraduate School
   Monterey, CA